Annual Scientific Image Contest Winners Album

ARVO®
The Association for Research in Vision and Ophthalmology

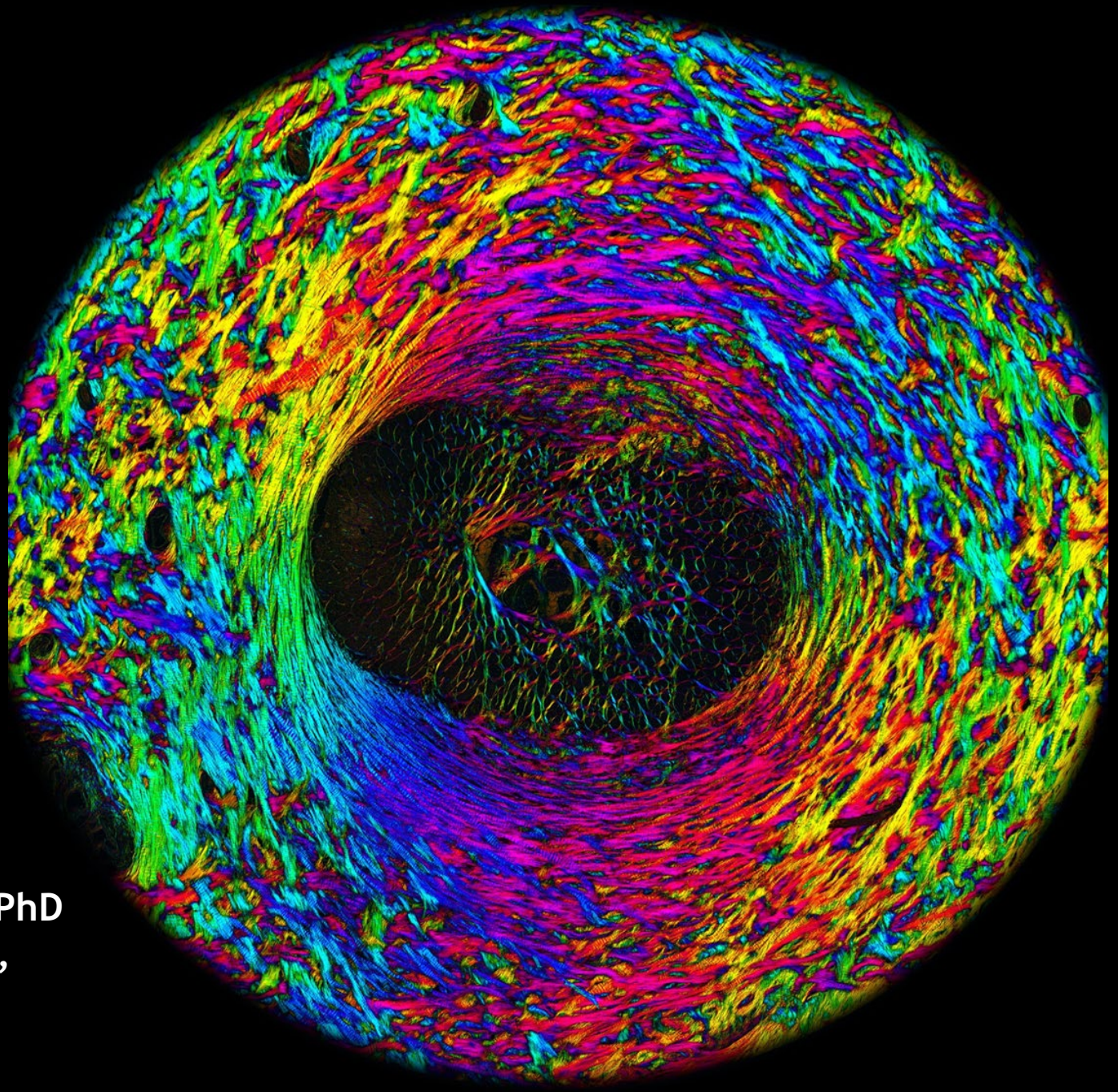

Image by Po-Yi Lee, PhD and Ian A. Sigal, PhD, FARVO

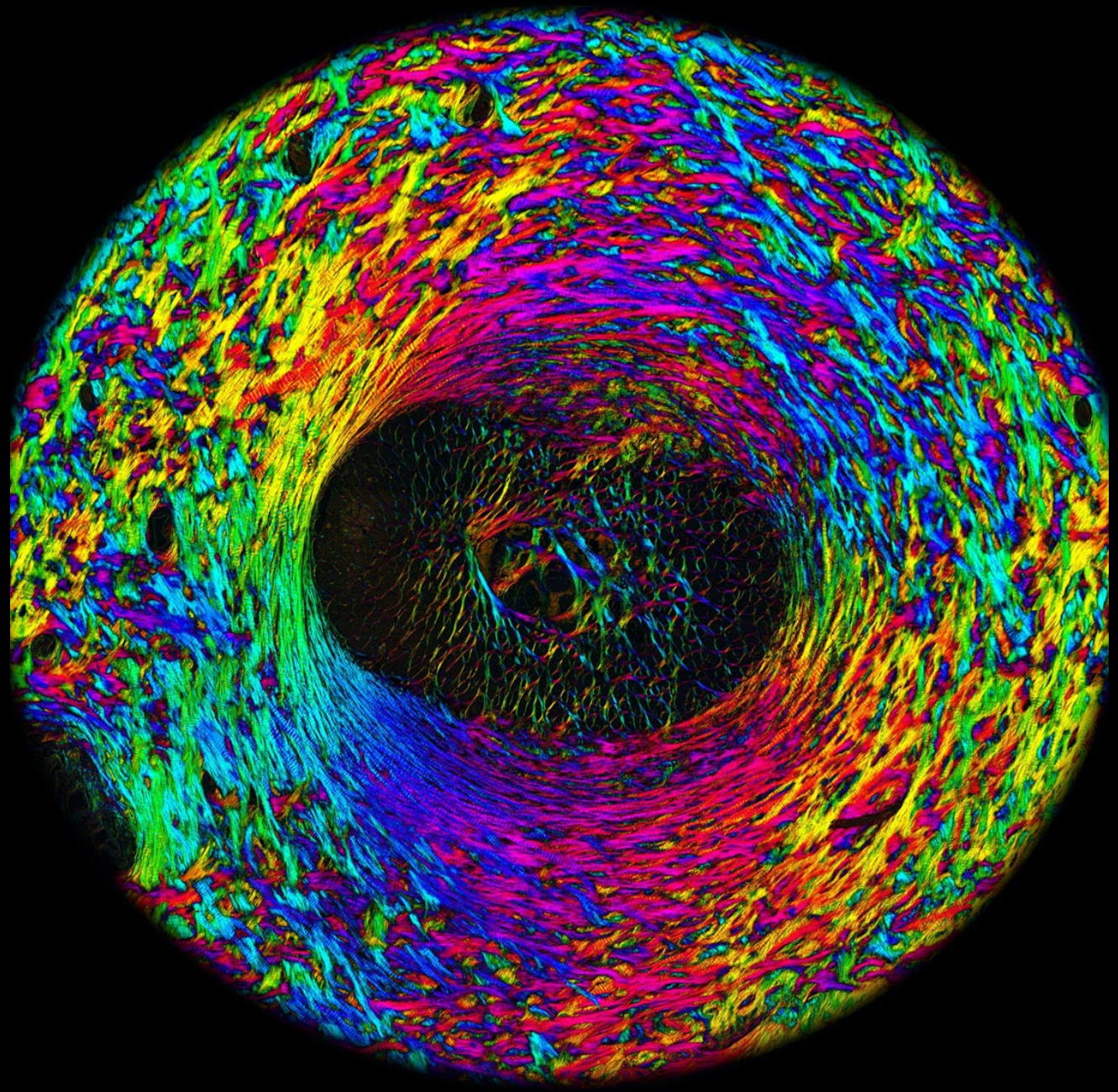

This image is a coronal section of a pig optic nerve head imaged by instant polarized light microscopy pi (IPOLπ). IPOLπ presents collagen fiber orientation and density in a color snapshot, with no need for labels, stains, or multiple image reconstruction. This color snapshot unveils the intricate collagen architecture within the optic nerve head, shedding light on the critical role of collagen in understanding ocular biomechanics.

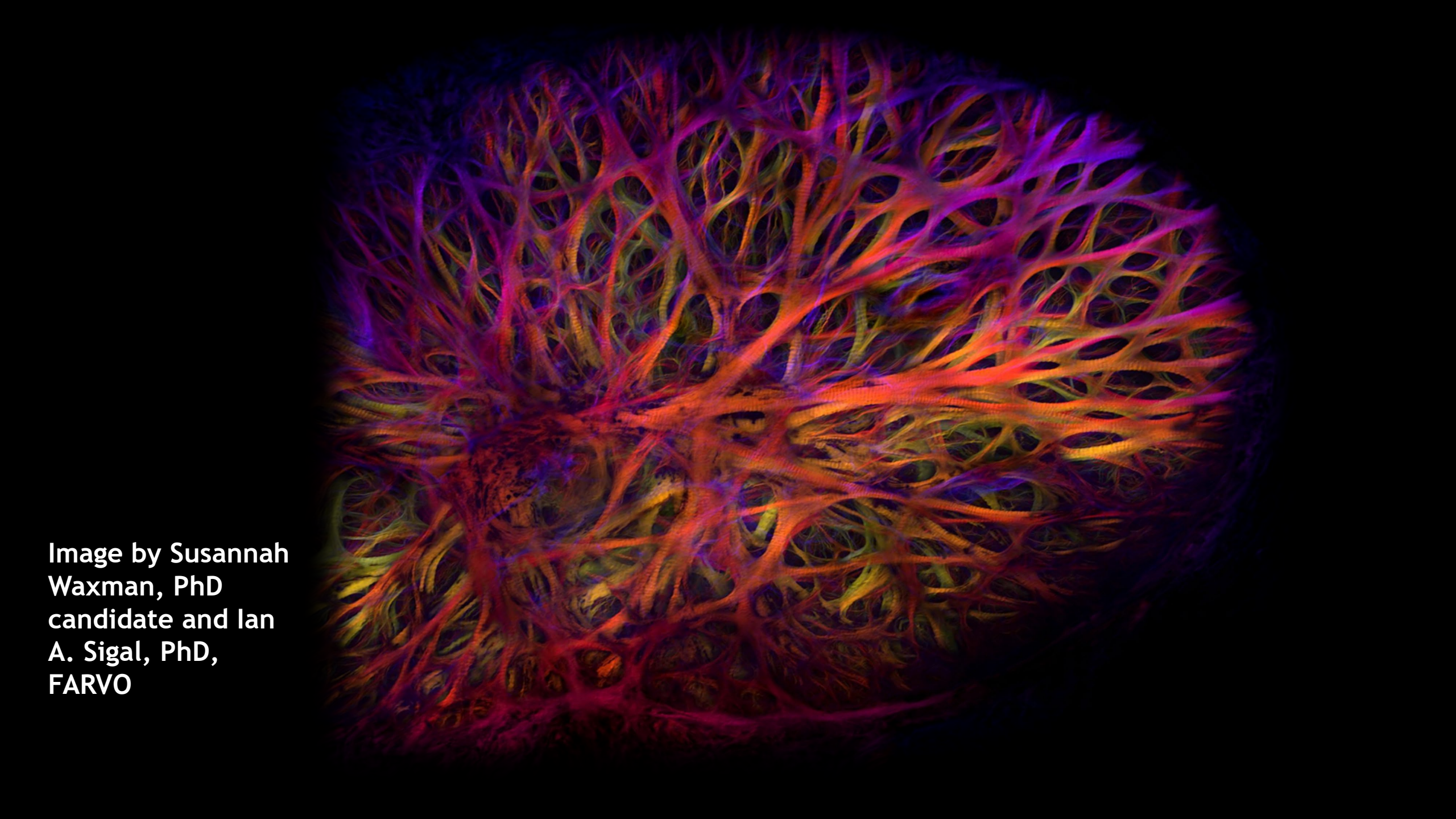

Image by Susannah Waxman, PhD candidate and Ian A. Sigal, PhD, FARVO

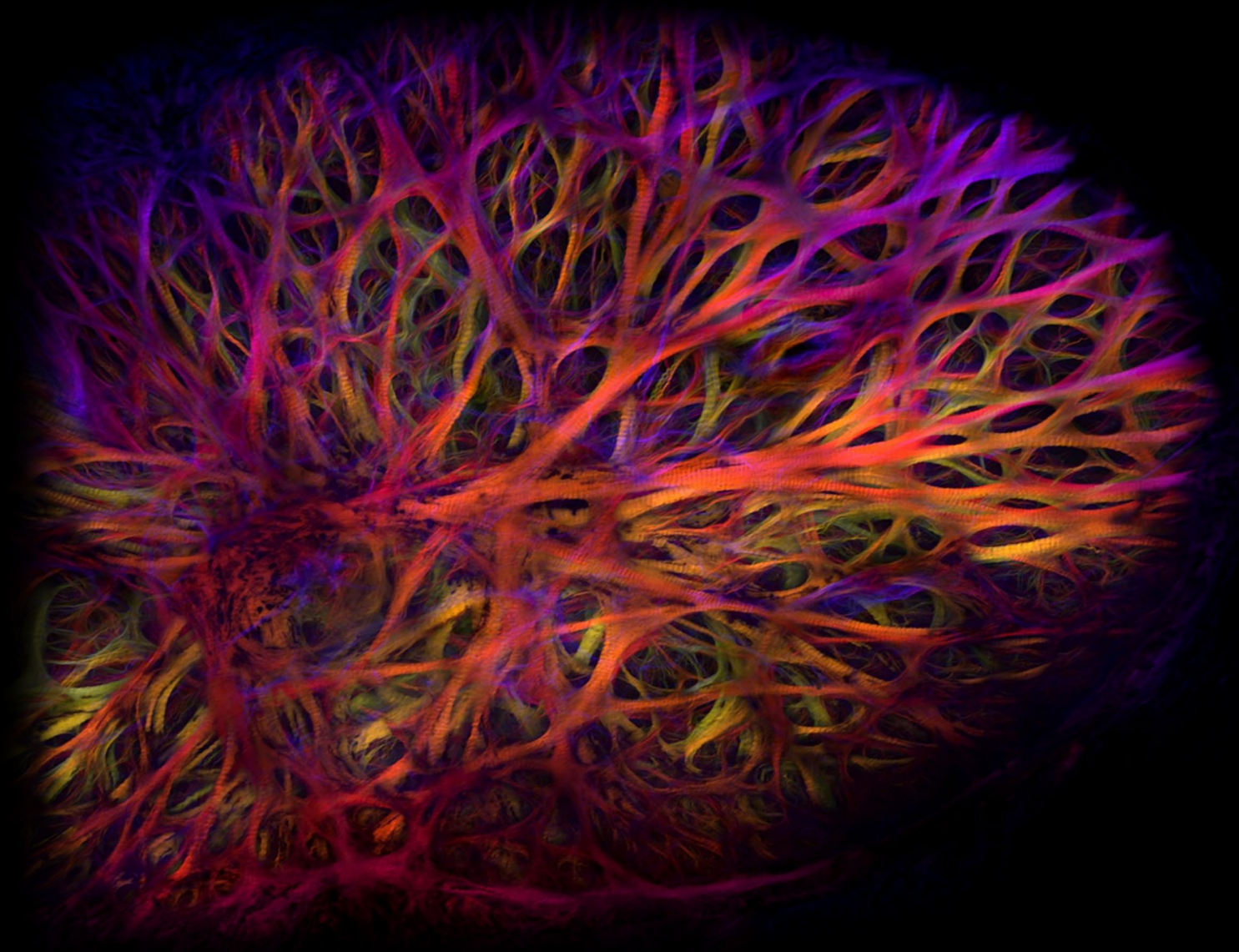

This image shows collagen of a sheep lamina cribrosa imaged with multiphoton microscopy. The colors represent depth, from purple in the anterior, red in the middle and yellow 450µm deep.

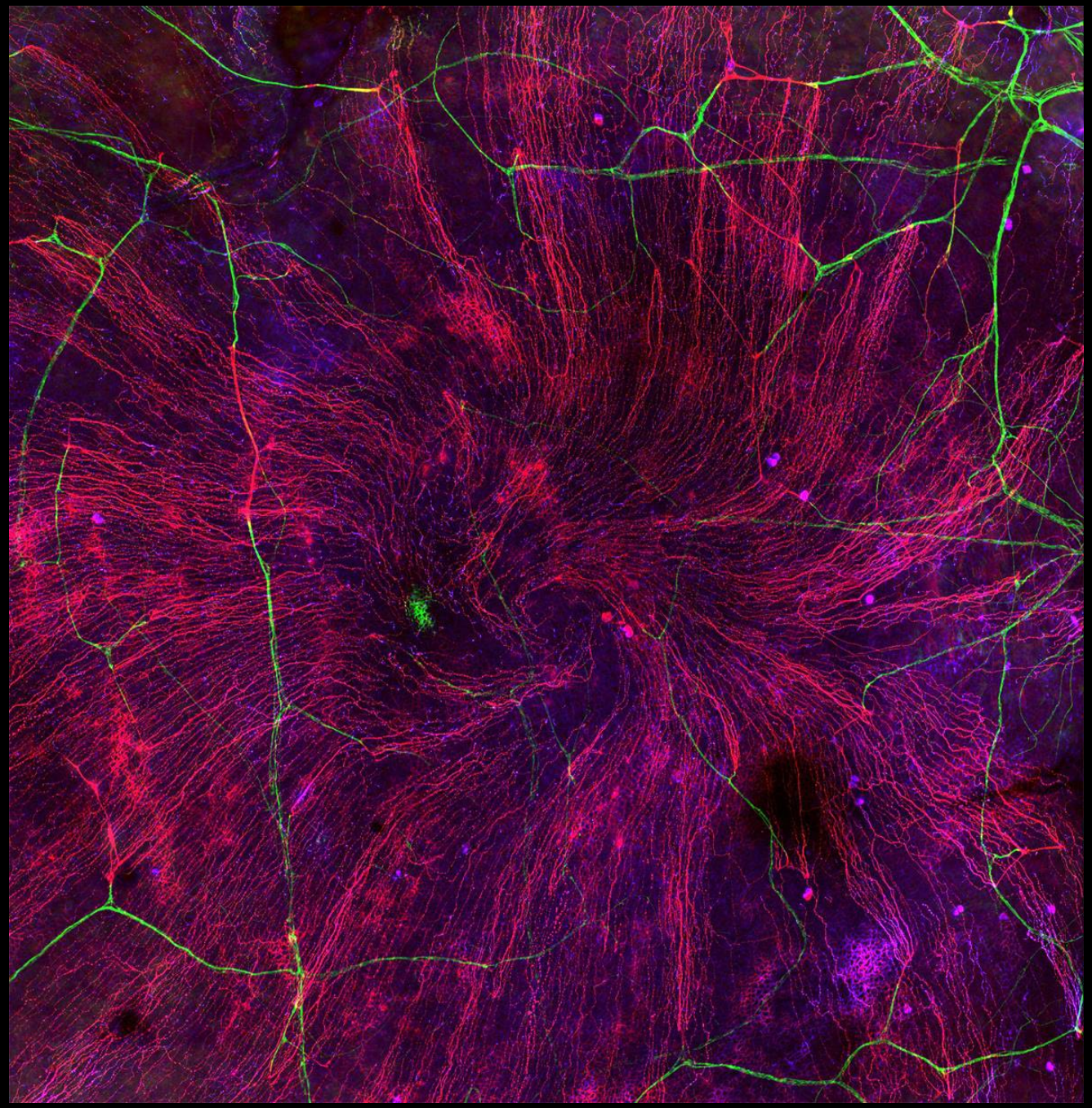

Image by Anton Lennikov, PhD, MD and Menglu Yang, PhD, MD

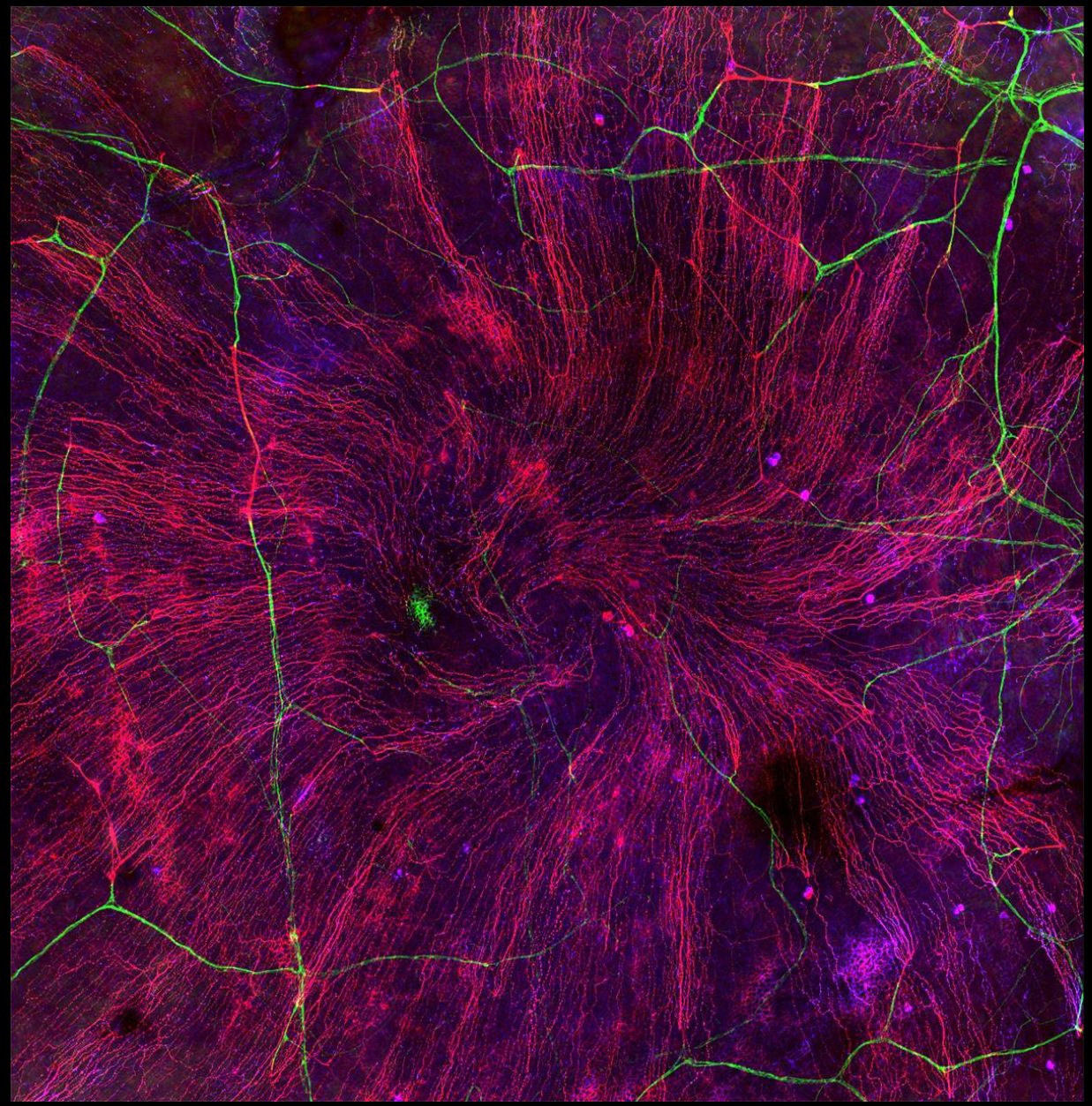

Mouse corneal nerves are visualized by beta-III-tubulin staining. Deep z-stack and tile scan image. Depth color coding: corneal nerve tips 0-3 um deep are colored in blue, 4-10 superficial corneal nerves are colored in red, and 10+ µm deep basal nerves are colored in green.

Image by Juana Gallar, MD, PhD, FARVO

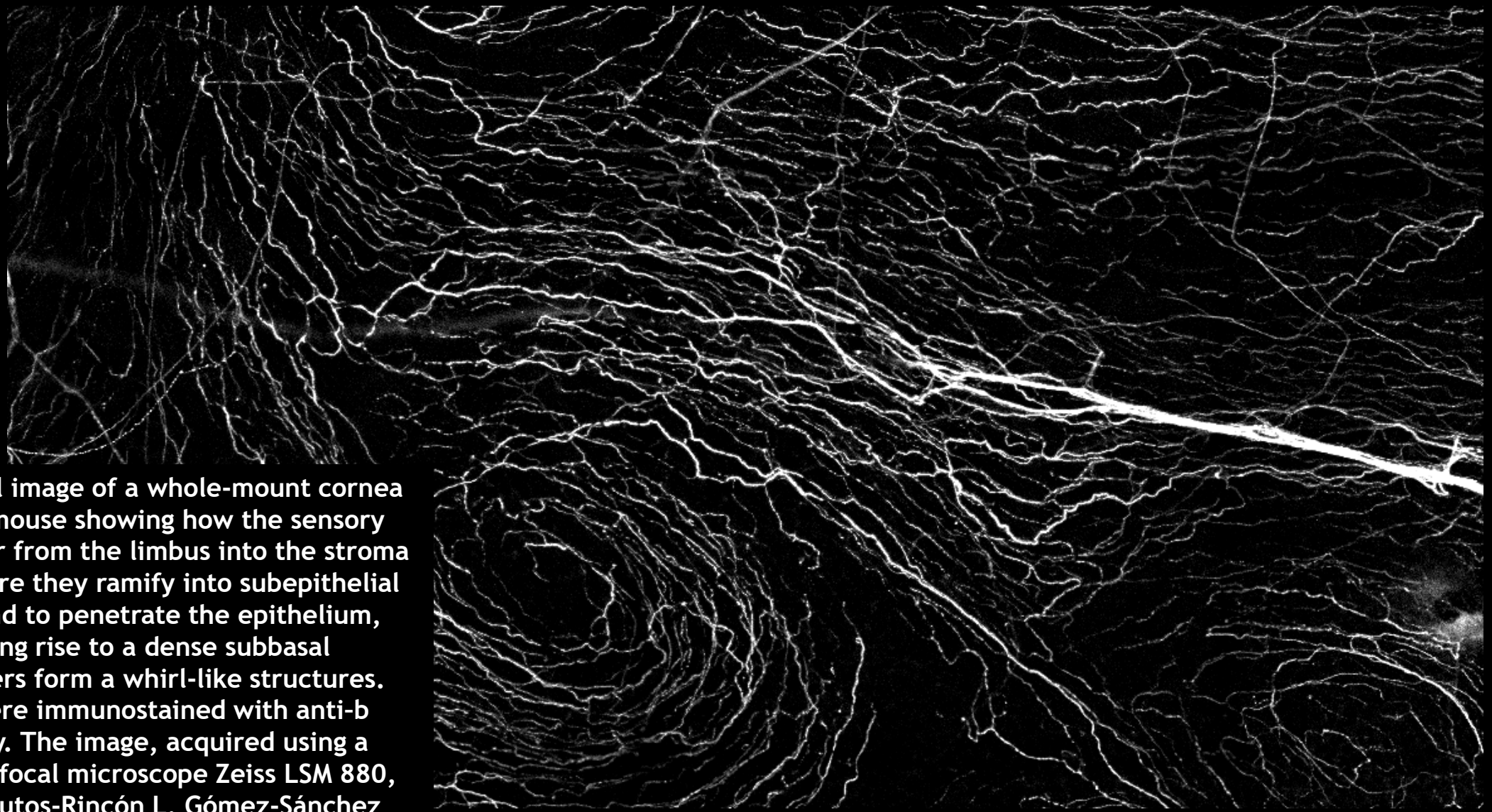

Z-stacked confocal image of a whole-mount cornea from a C57BL/6J mouse showing how the sensory nerve trunks enter from the limbus into the stroma of the cornea where they ramify into subepithelial fibers which ascend to penetrate the epithelium, branching and giving rise to a dense subbasal plexus, whose fibers form a whirl-like structures. Corneal nerves were immunostained with anti-b tubulin III antibody. The image, acquired using a laser scanning confocal microscope Zeiss LSM 880, was included in Frutos-Rincón L, Gómez-Sánchez JA, Íñigo-Portugués A, Acosta MC, Gallar J (2022). https://doi.org/10.3390/ijms23062997.

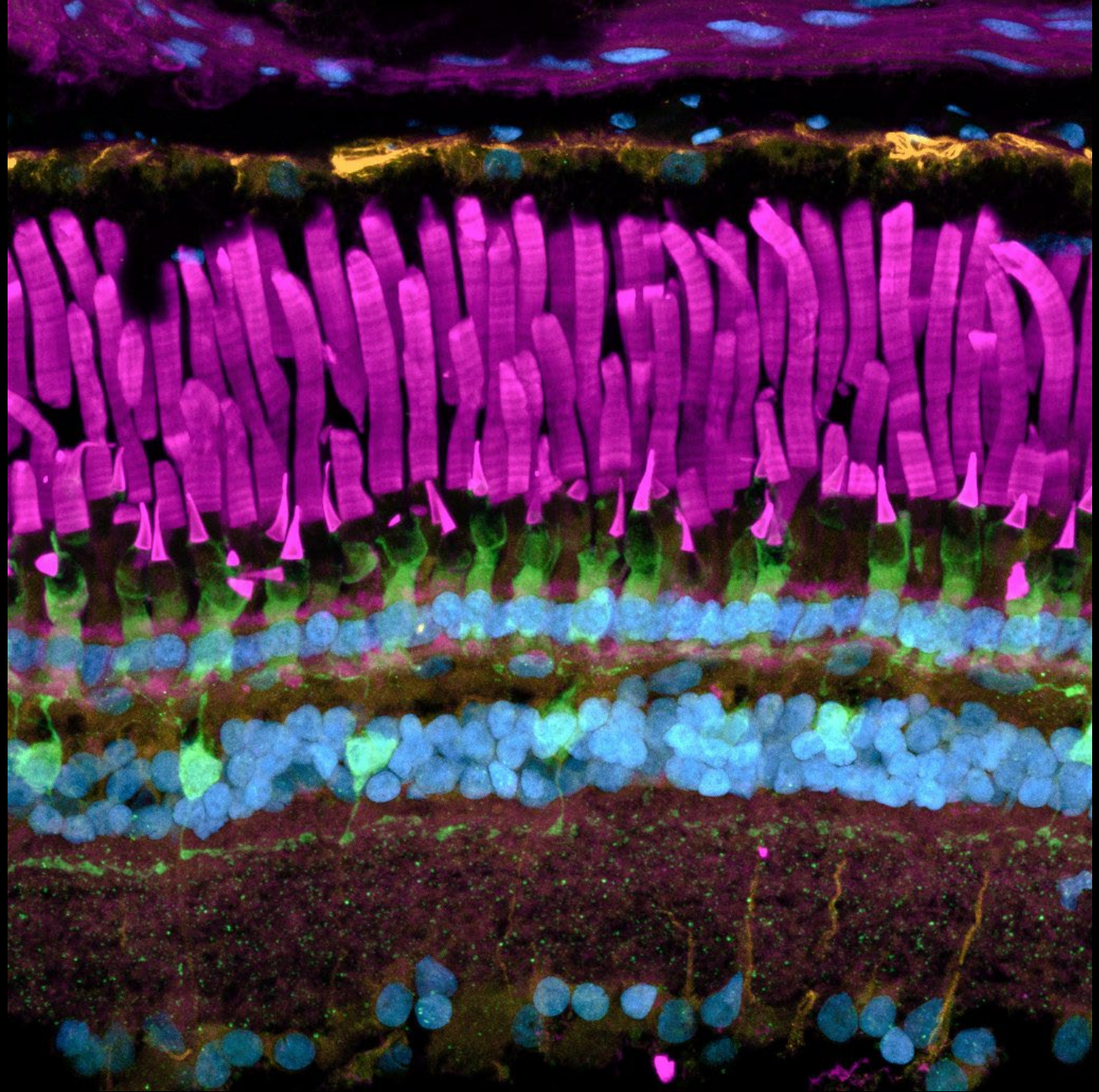

Image by
Brittany Carr,
PhD

This is a Xenopus laevis retina labeled with wheat germ agglutinin (photoreceptor outer segments; magenta), vimentin (glia & cytoskeleton components; orange), calbindin (bipolar cells and cone inner segments; green), and Hoechst (nuclei; light blue). This image is a great example of the structure and laminations of the retina; it demonstrates some of the variety of cell types that can be labeled in the healthy Xenopus eye. I use these antibodies to investigate and track photoreceptor degeneration and deteriorating retinal health in genetically modified frogs created to model cone-rod dystrophy and macular degenerative disease. This micrograph was created using immunohistochemistry and was imaged on a Zeiss LSM 800 confocal microscope.

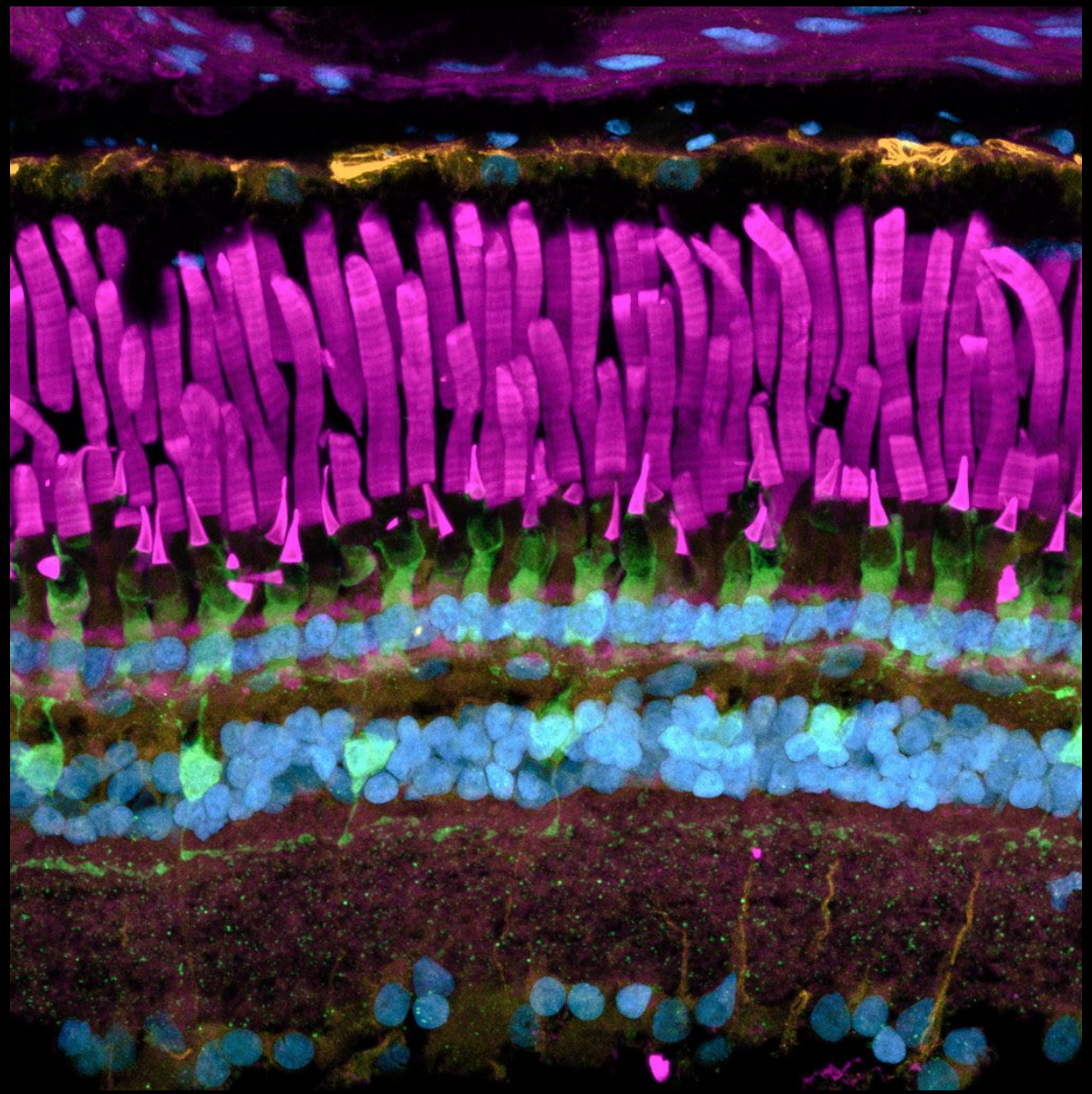

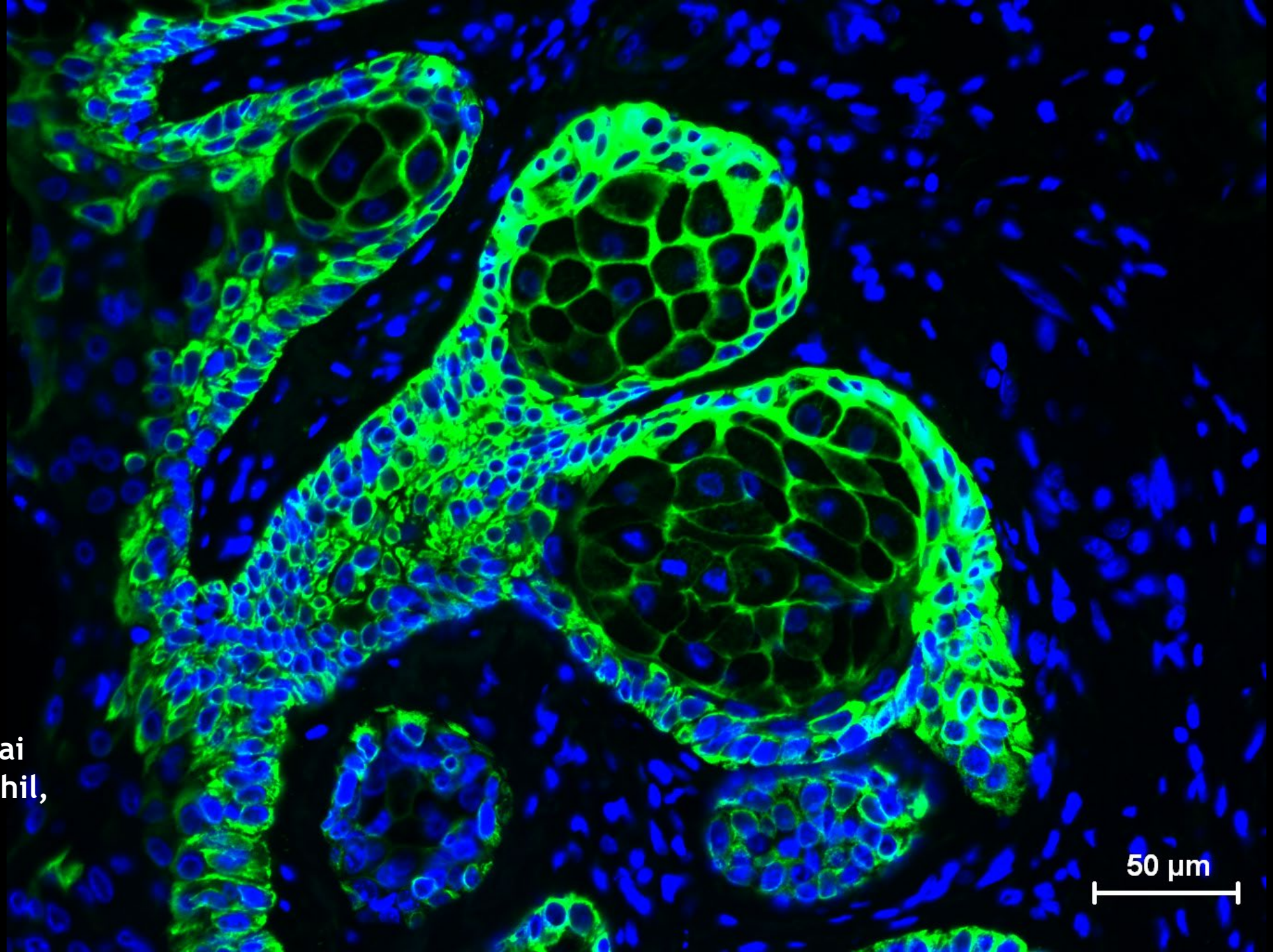

Image by Jingna He, PhD, and Wai Kit Chu, MPhil, DPhil

This is an image of human meibomian gland tissue stained with the cytokeratin 14 antibody. Cytokeratin 14 signals were detected in both the meibocytes (lipid containing cells), the ductuli (smaller ducts connecting the meibocytes and the central duct) and the central excretory duct, suggesting an epithelial origin of these cells.

Techniques: A human eyelid tissue was fixed and sectioned. Immunohistochemical staining of cytokeratin 14 (green) is shown. DNA was stained with DAPI (blue). The image was captured by using a fluorescence microscope.

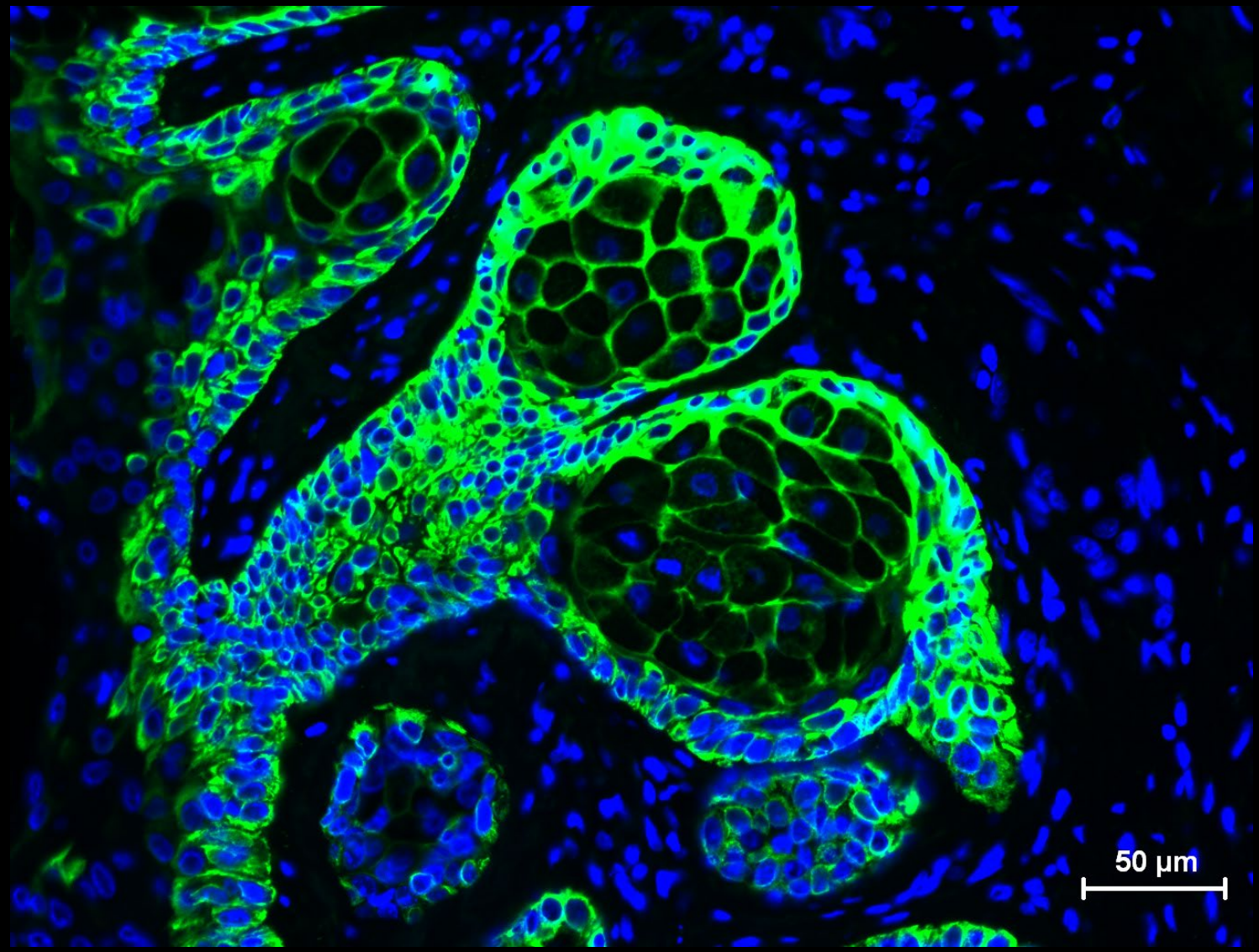

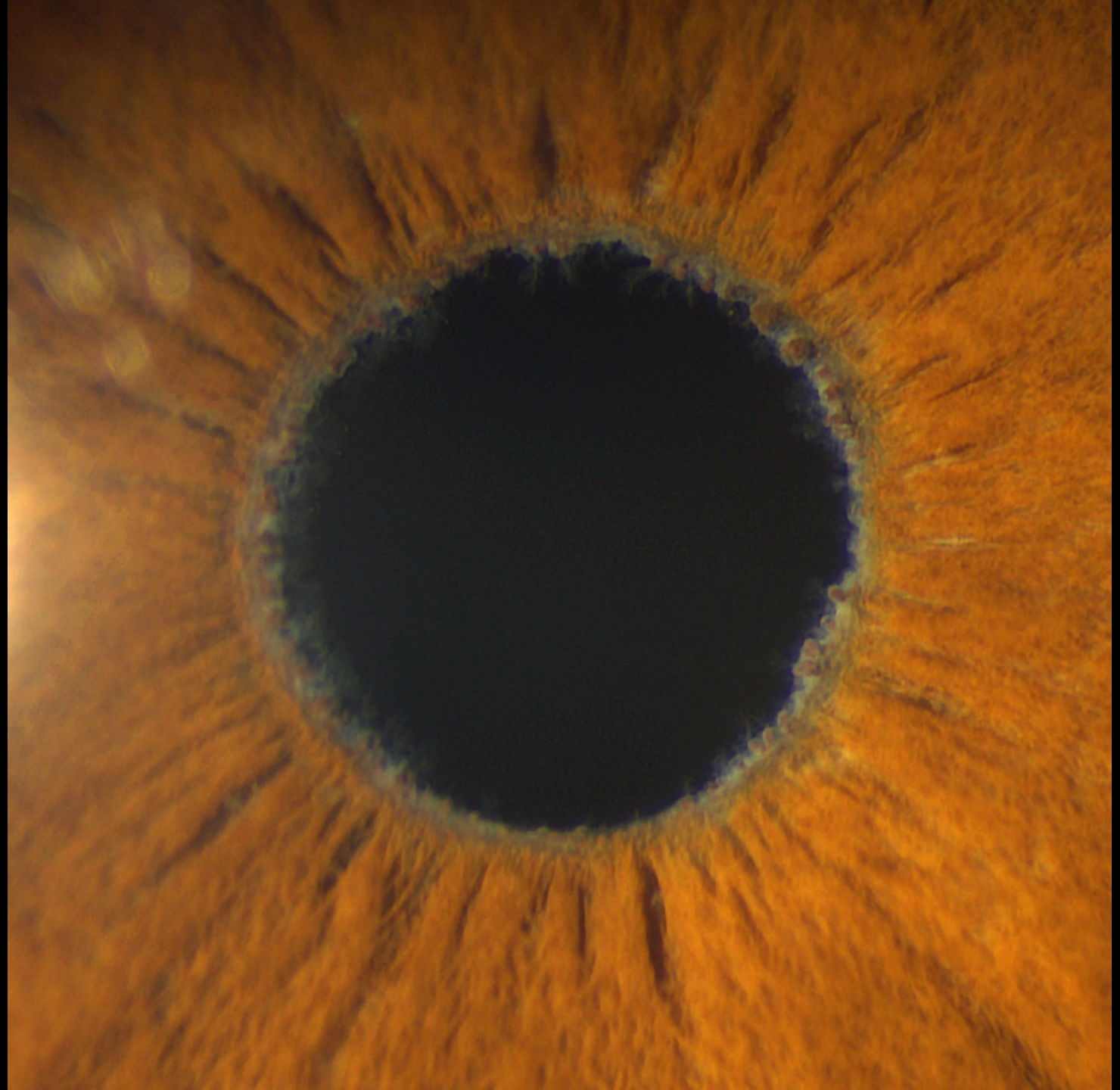

Image by Joel S. Schuman, MD, FARVO

This 90-year-old pseudophakic patient with pseudoexfoliation syndrome had a striking decoration of the pupillary border with pseudoexfoliation material. Techniques used to generate it: slit lamp photography

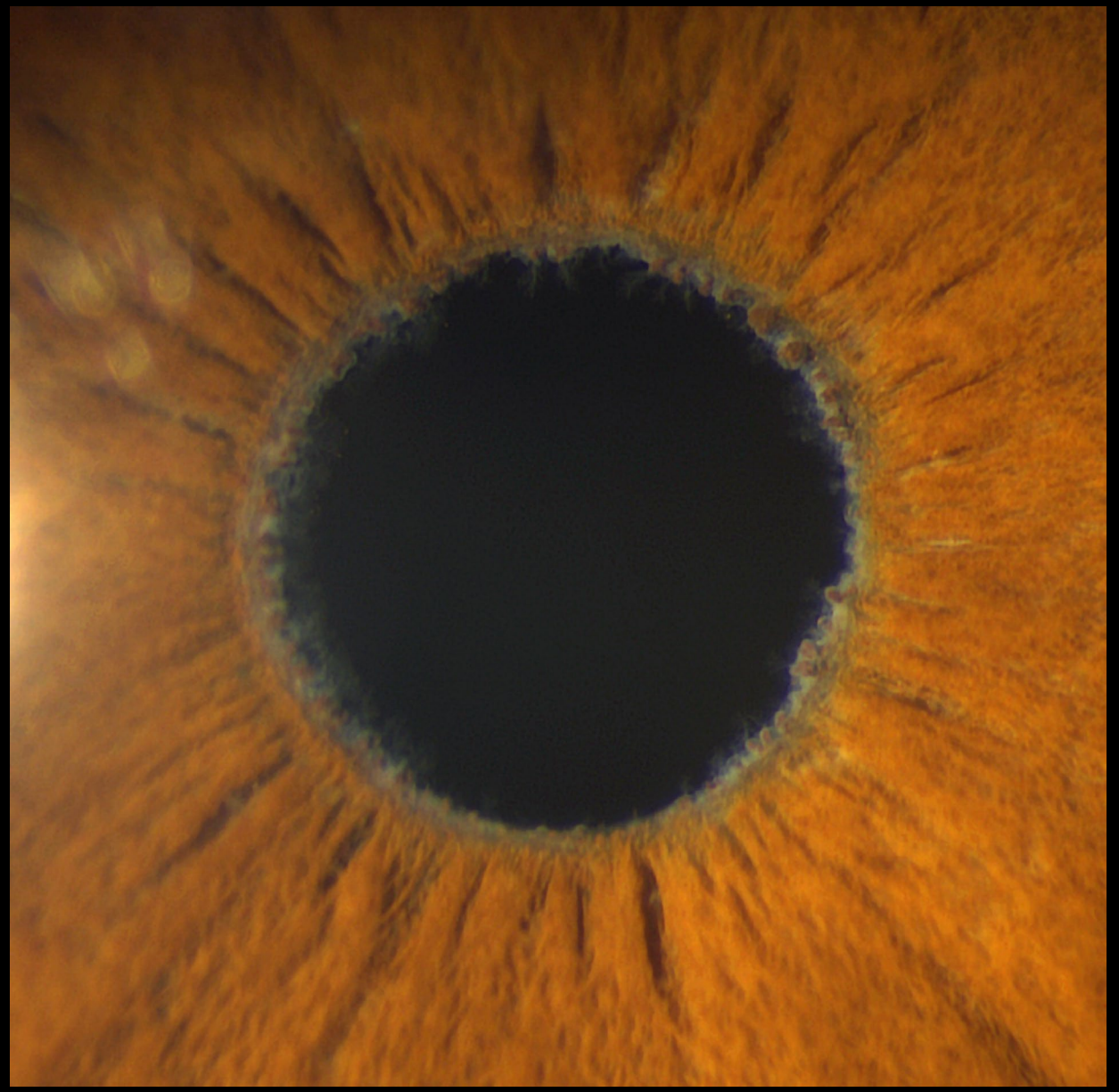

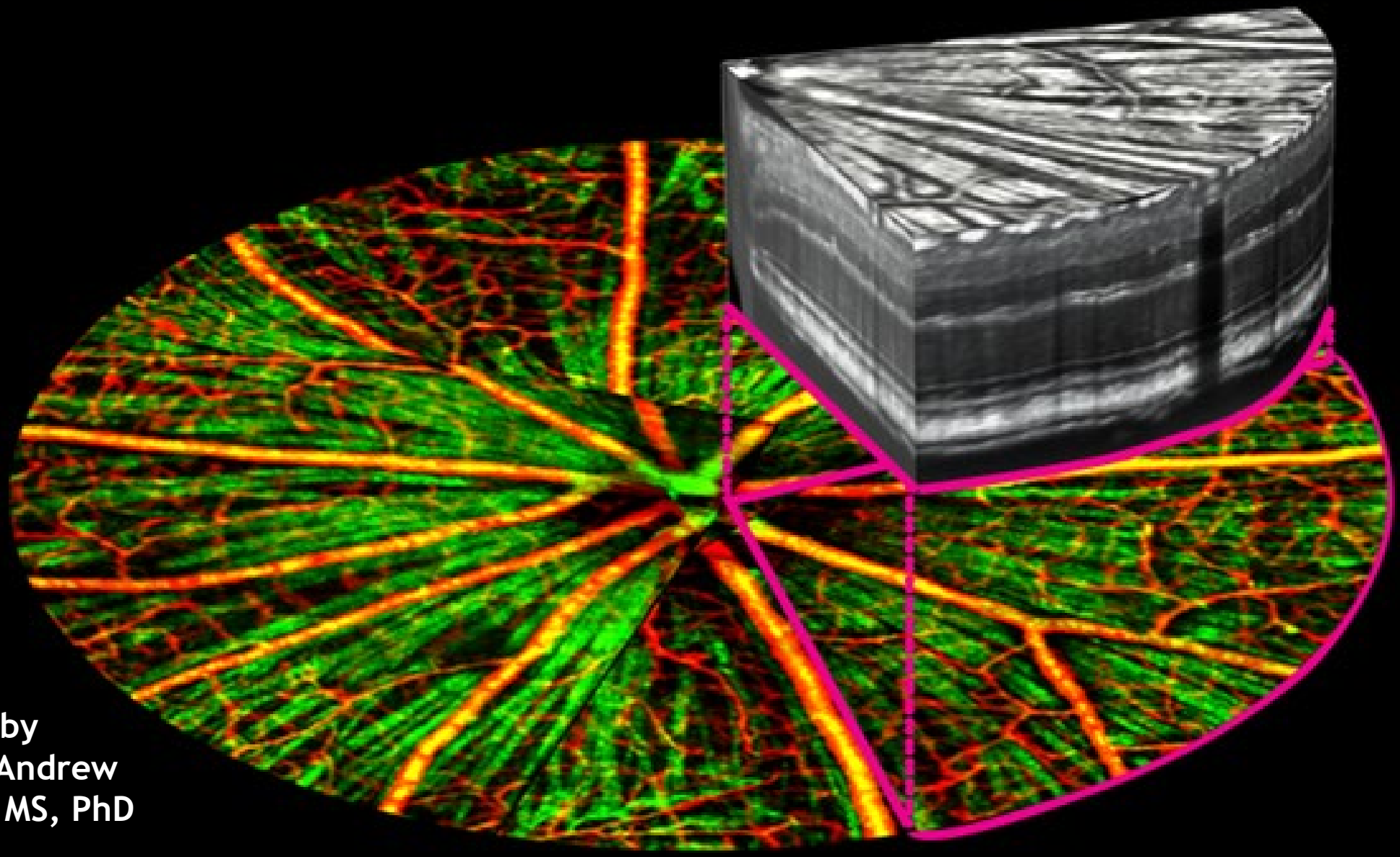

Image by
David Andrew
Miller, MS, PhD

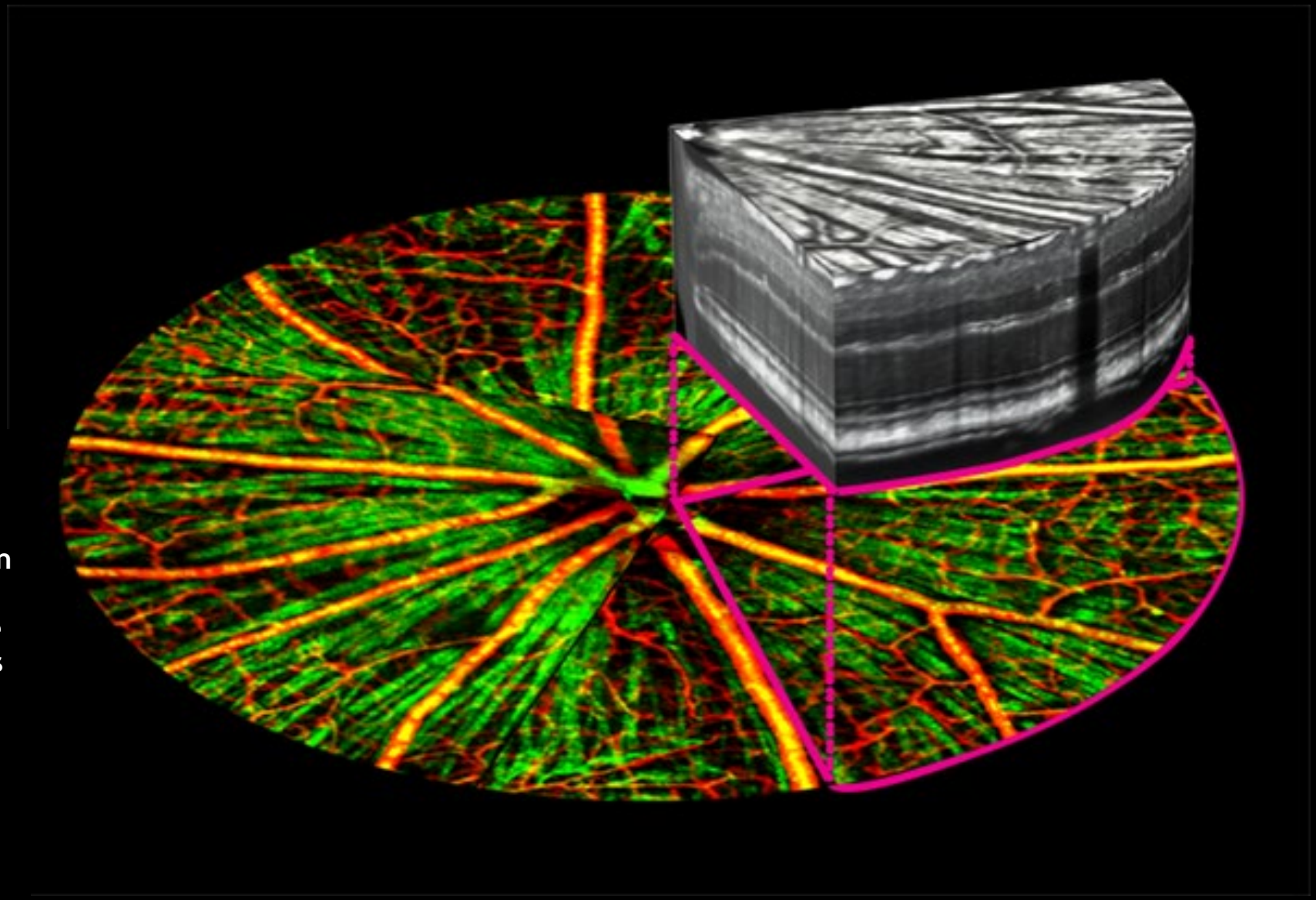

This slice of the mouse retina was captured by visible-light optical coherence tomography fibergraphy (vis-OCTF). Using this method, we can clearly visualize the RGC axon bundles located on the surface of the mouse retina. This technique enables a more holistic evaluation of bundle health by visualizing changes in bundle morphology in response to different disease conditions.

Technique: Visible-light optical coherence tomography fibergraphy

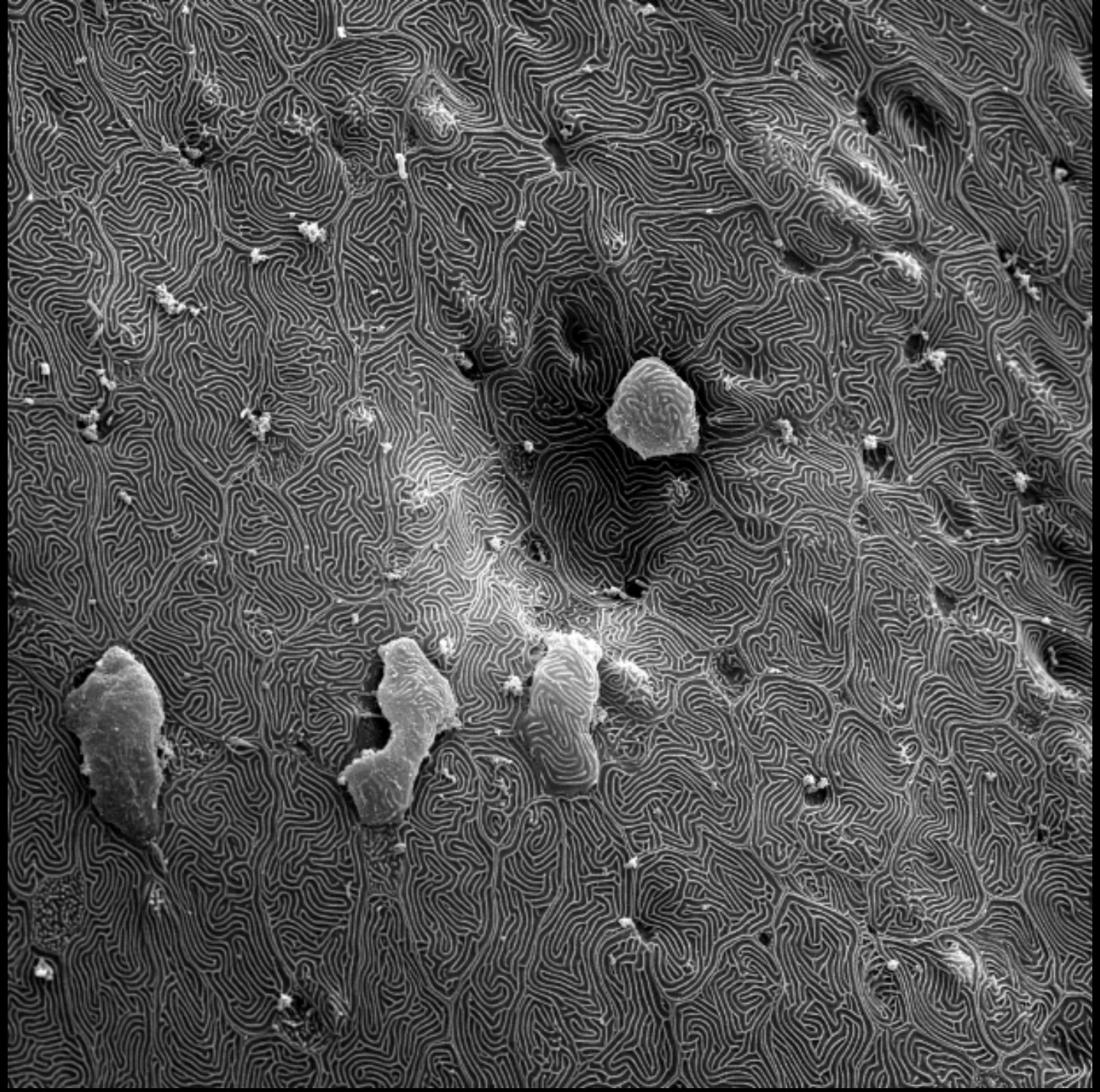

Image by
Justin Courson,
PhD

This scanning electron microscopy image depicts the epithelial surface of an adult zebrafish (Danio reirio) cornea. Human epithelial cells form ridges, or microplicae, which are often disorganized in appearance. However, the microplicae of zebrafish epithelial cells form intricate ridges that assume a maze-like appearance. Despite this striking difference in form, both species depend on surface epithelium to protect corneal integrity and maintain ocular transparency. This includes a constant turnover of superficial squamous cells which assume a rounded appearance before being sloughed off, exposing younger underlying cells. In this image four such cells can be seen detaching from the surface, and, upon closer inspection, newly exposed cells can be seen peeking through the borders between overlying cells. Field size: 88 x 88 µm

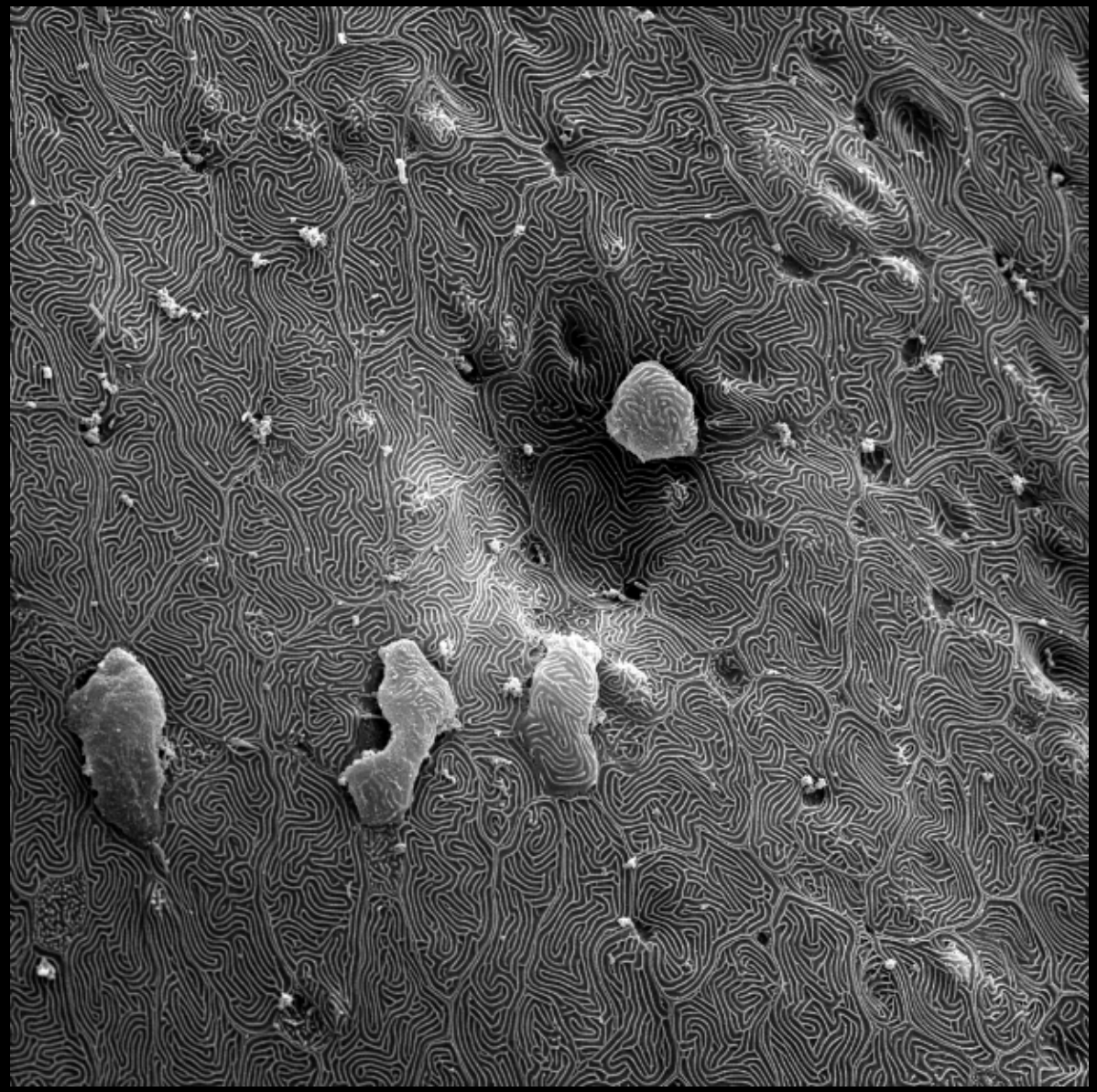

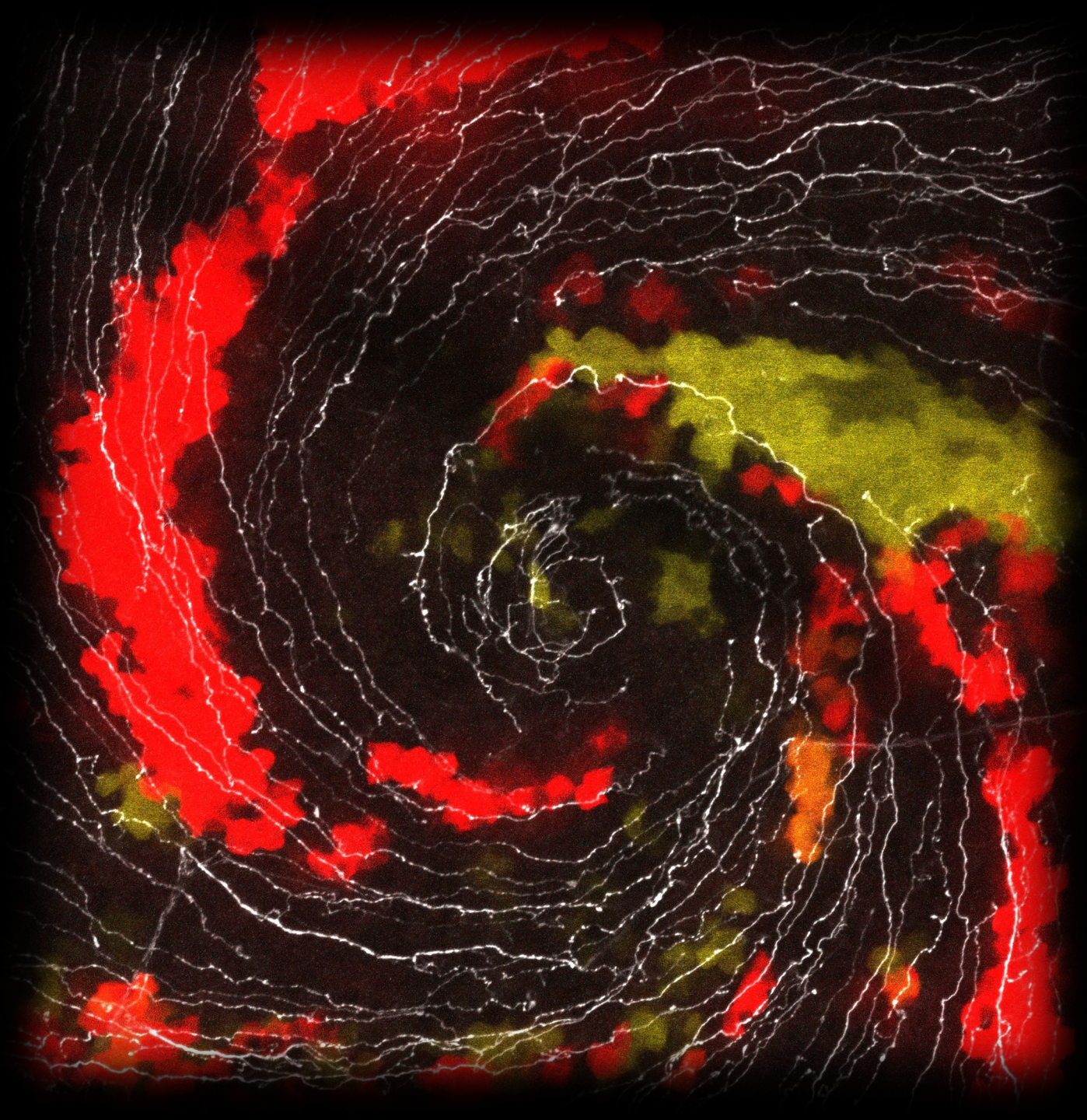

Image by
Nick Di
Girolamo, PhD

Interactions between sensory neurons and epithelial cells within the mammalian cornea are intriguing but difficult to discern. Our goal is to determine whether this association can be used to glean the health status of the cornea under a myriad of conditions. This fluorescence confocal microscopy image captures the visual association between the intraepithelial corneal basal nerve plexus (white trace) with multicolored corneal epithelial cell migratory tracks in a K14CreERT2-Confetti biosensor mouse. The cornea was collected 20-weeks post-tamoxifen administration then immunostained for ßIII-Tubulin. The image represents a maximum intensity projection taken from the paracentral zone where both cellular components twist in the same direction to form a distinct whorl.

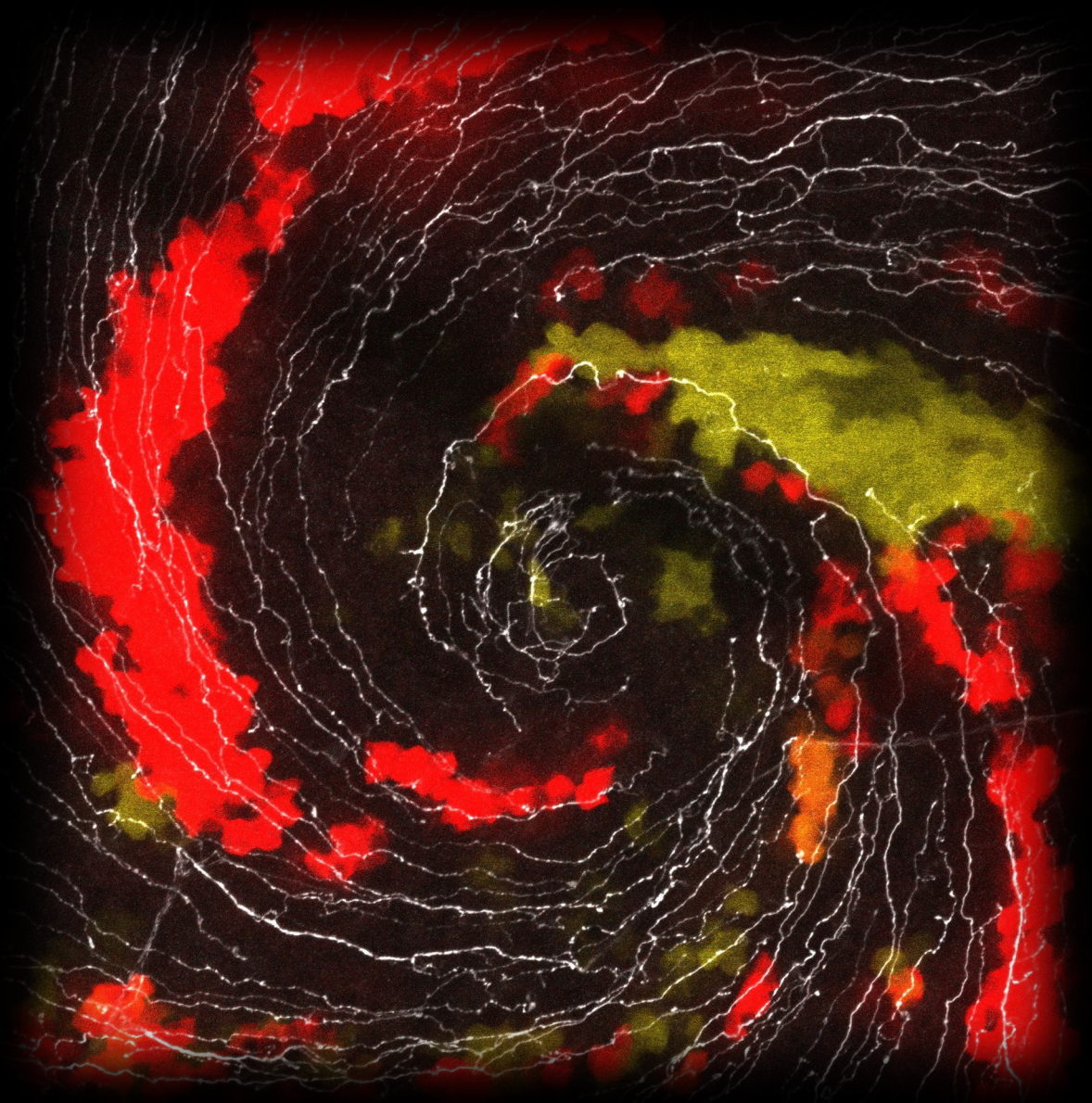

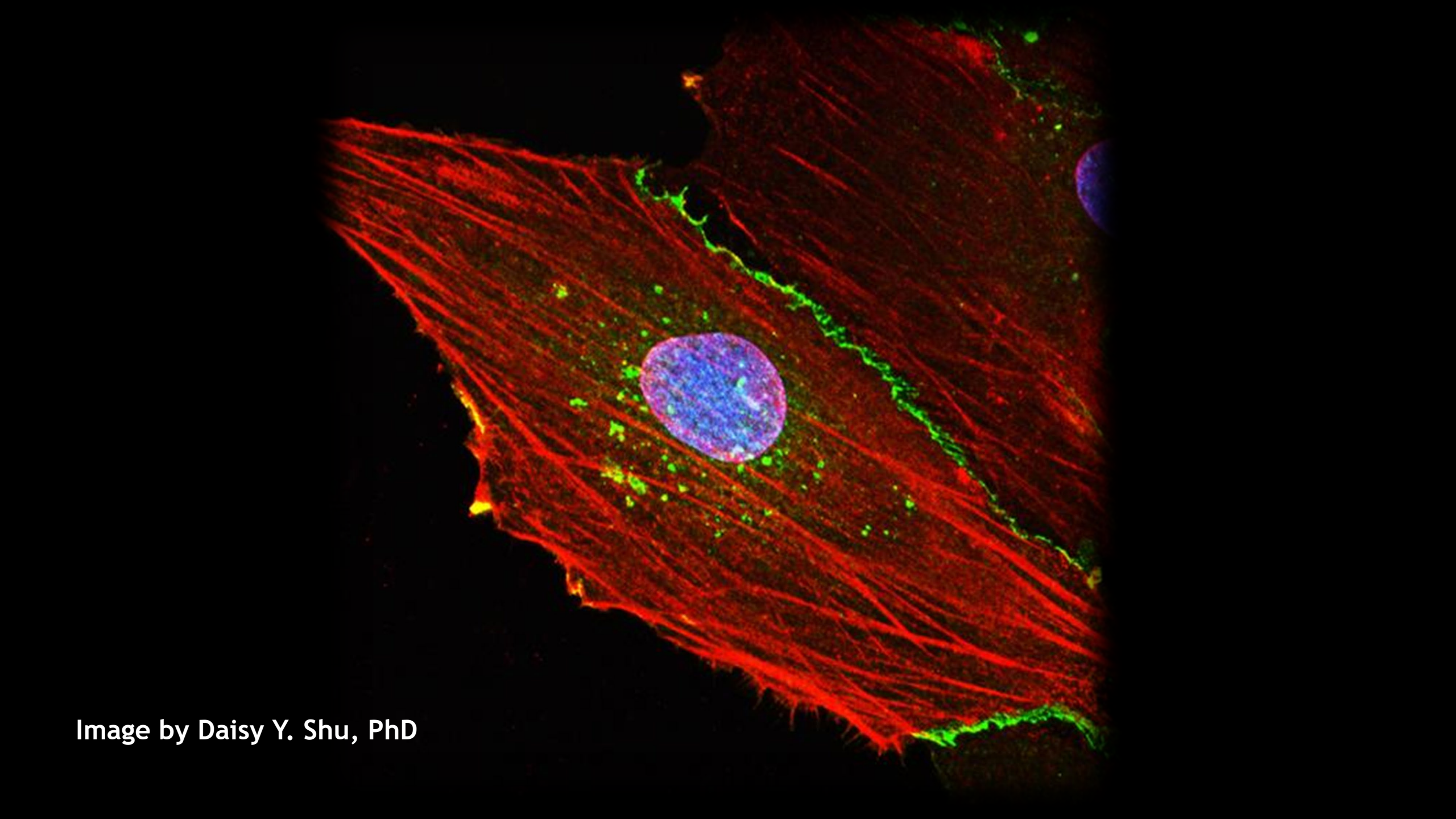

Image by Daisy Y. Shu, PhD

During epithelial-mesenchymal transition (EMT), epithelial cells lose their polarity and transdifferentiate into motile and contractile mesenchymal cells. This process involves a re-organisation of the actin cytoskeleton into dynamic stress fibres enabling cells to transmit contractile forces. Here we see human lens epithelial cells that have undergone EMT following treatment with transforming growth factor-beta (TGFß). The cells exhibit strong immunoreactivity for the mesenchymal marker, alpha-smooth muscle actin (red), localising to stress fibre bundles and a concomitant translocation of the epithelial marker, beta-catenin (green) from the membrane to the peri-nuclear region. The nucleus is stained with Hoechst (blue). Taken on a Zeiss LSM-5Pa confocal microscope.

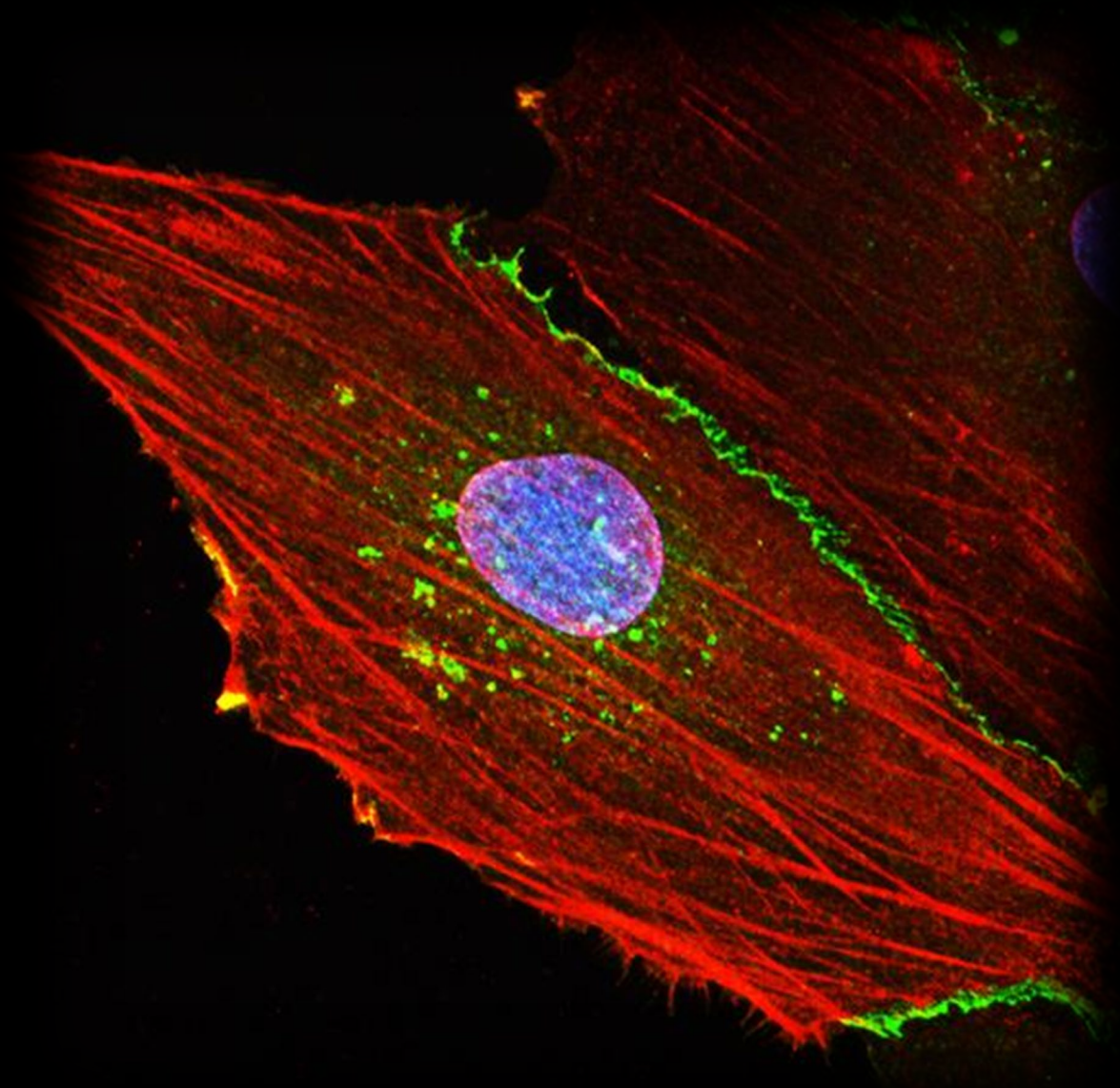

Image by Michael Lovelace, PhD, and Tailoi Chan-Ling, BOptom, PhD, FAAO, FARVO

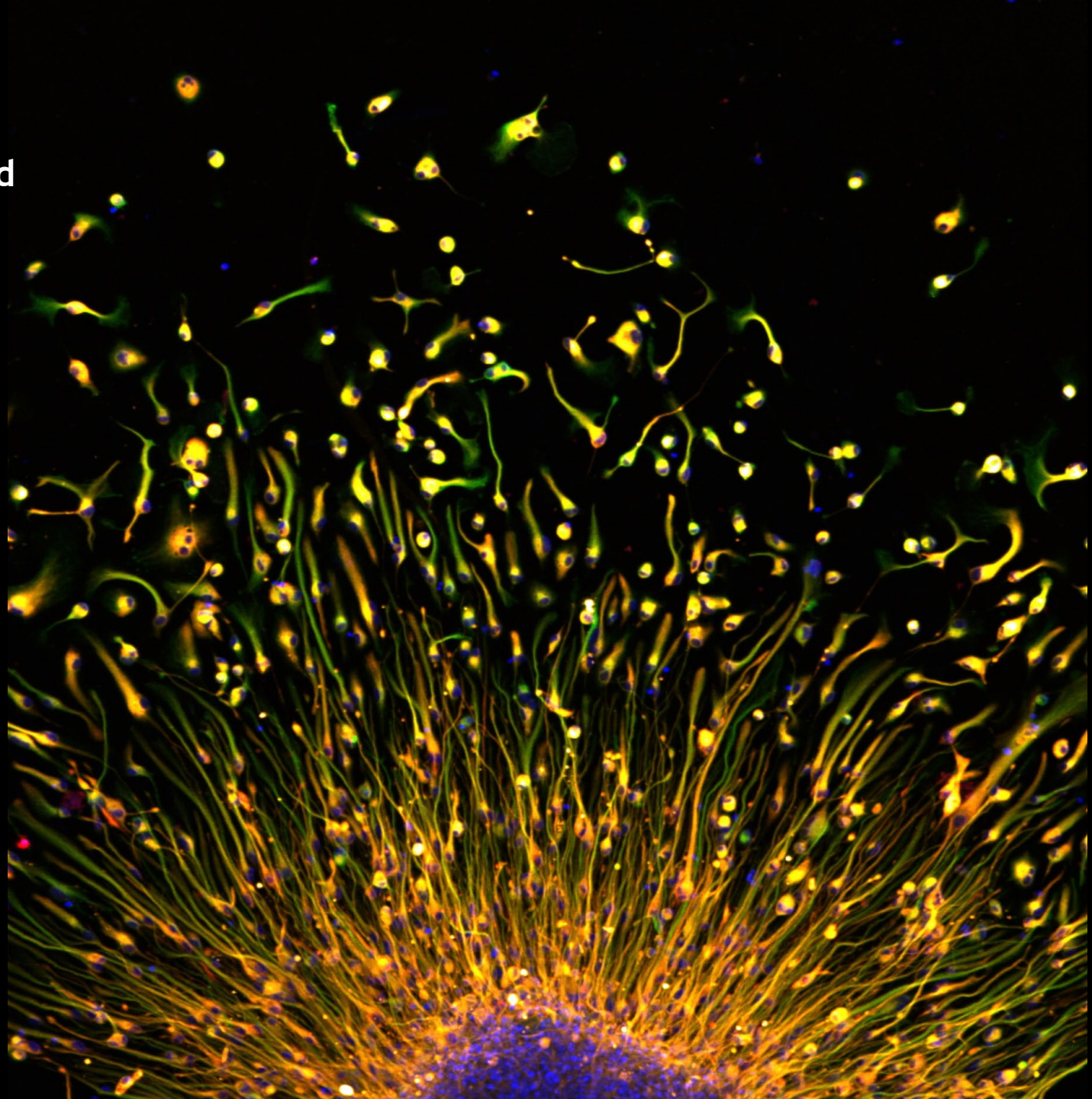

Like a spectacular dawn sunrise, this image of human neural precursor cells illustrates the complexity of morphologies and markers expressed on immature cells as they migrate and show a more differentiated phenotypes. This image formed part of a novel study where we demonstrated that human neural stem cells highly expressed the P2X7 purinergic receptor (which functions as a phagocytic scavenger receptor in the absence of extracellular ATP), and plays a major role in phagocytosing apoptotic neural cells due to excess production during brain development (Lovelace MD, Chan-Ling T et. al, "P2X7 receptors mediate innate phagocytosis by human neural precursor cells and neuroblasts", Stem Cells 33(2), (2015) pp. 526-541; Pubmed ID 25336287). This work provided the groundwork for other labs' who showed a role for loss of P2X7 in AMD. Collectively, these findings underlie the importance of phagocytosis by P2X7 during neurodevelopment and in the aging visual system.

As we watched the neurospheres, we were struck by the natural beauty of the structure. The resultant image is a culmination of advanced confocal microscopy and a 6 marker immunofluorescence technique pioneered in our lab (Mansour et al 2013 PLoS One). The colours in the image represent differential expression of stem or precursor cell markers as the cells stochastically begin differentiating.

This micrograph was taken using a Zeiss LSM confocal microscope, with a final magnification of 100x and image resolution of 2048x2048 pixels, and is represented as a z-projection of multiple slices acquired as a z-stack in each of the 4 laser channels, in order to reconstruct the 3D neurosphere structure and cell inter-relationships, and also single, migrated cells in the monolayer.

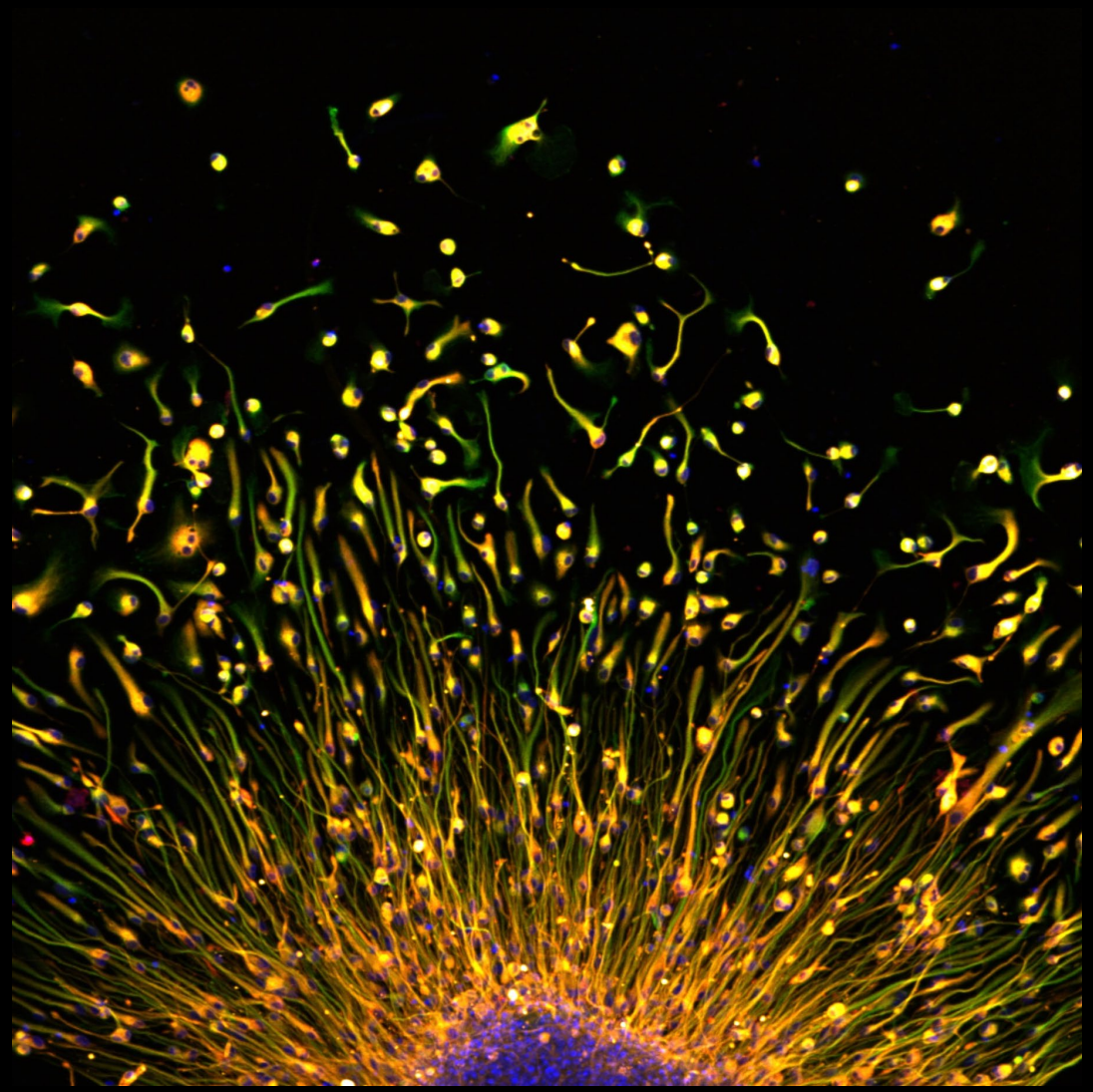

Image by Christina Mastromonaco, PhD, MSc

Yearly 20 million people go blind from cataracts, as their aging lens becomes cloudy. Surgical advances allows for replacement of the natural lens with an artificial lens (an intraocular lens [IOL]). However, roughly 20% of the patients post-surgery will develop a secondary cataract (or posterior capsule opacification [PCO]), obstructing vision once again. Different designs and materials of IOLs exist, some more prone to PCO. Thus, we believe it is of great value to identify which IOL characteristics are more prone to PCO in order to reduce this vision-threatening complication. Our image allows visualization of the IOL implant (centered) within the structures of anterior half of the human eye. PCO formation (in grey) is observable around the IOL. These images are used to quantify PCO using custom software, allowing for a comparison between different IOL characteristics.

Our images are obtained using the Olympus DSX110 Digital Microscope. This microscope was primarily designed for quality control of microchips in industry. Due to its high-resolution image quality, we decided to use it on biological samples for the first time. A refined methodology was designed to establish the best quality images for these samples. No changes were made to our image.

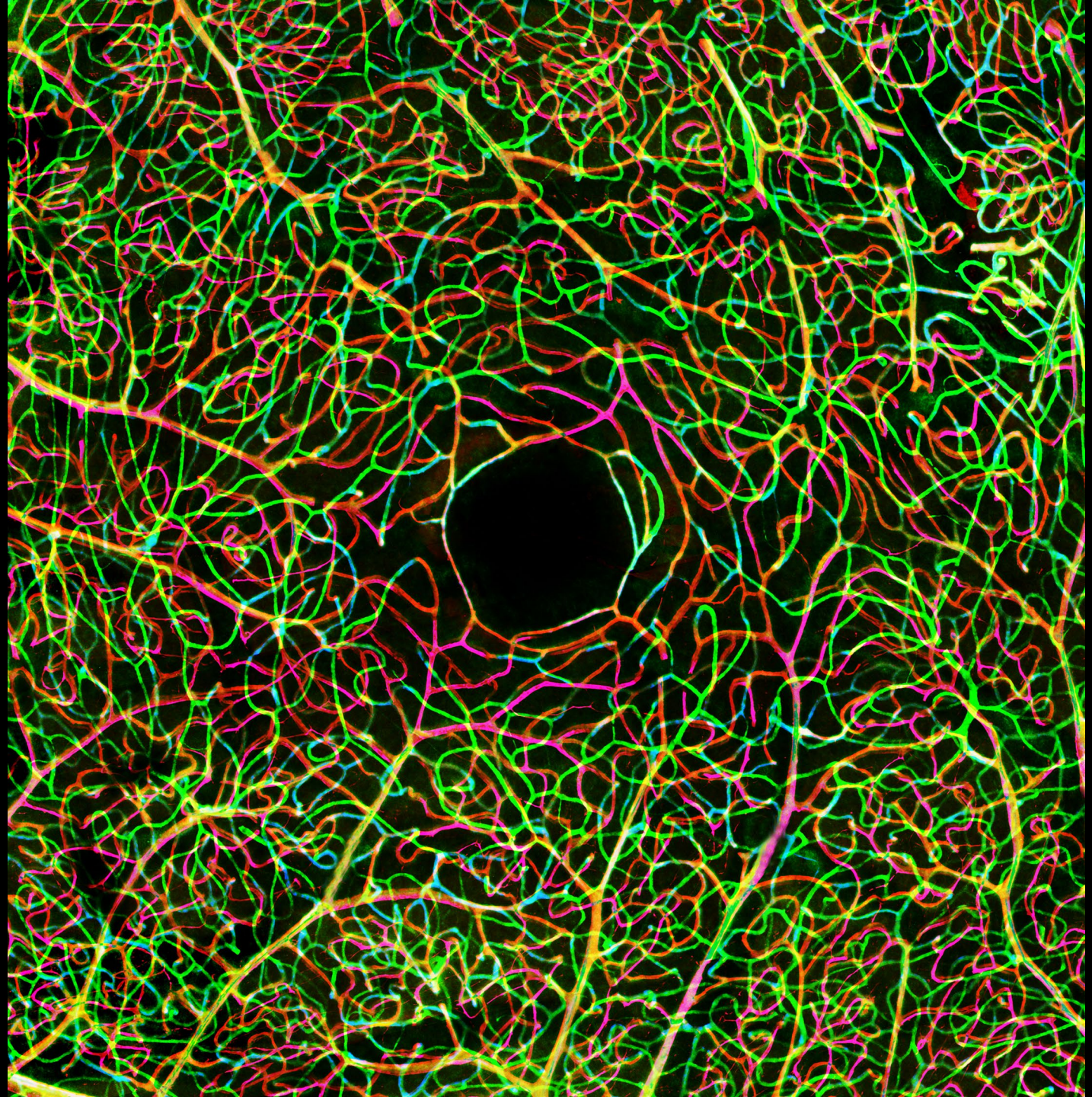

Image by Isabel Ortuño Lizarán, PhD and Nicolás Cuenca, PhD

Vascular plexus of a post mortem human retina in the macula. The central region, absent of blood vessels, is the foveal avascular zone. Each vascular plexus is represented in a different color…in this work, we aim to analyze the vascular plexus of post mortem human retina to describe the normal state of retinal blood vessels and the changes that occur associated with different pathologies.

We performed immunohistochemistry using antibodies specific to collagen-V and confocal imaging in a Leica SP8 confocal. Each vascular plexus was obtained as a separate image and they were merged into a single image. Each plexus is represented in a different color.

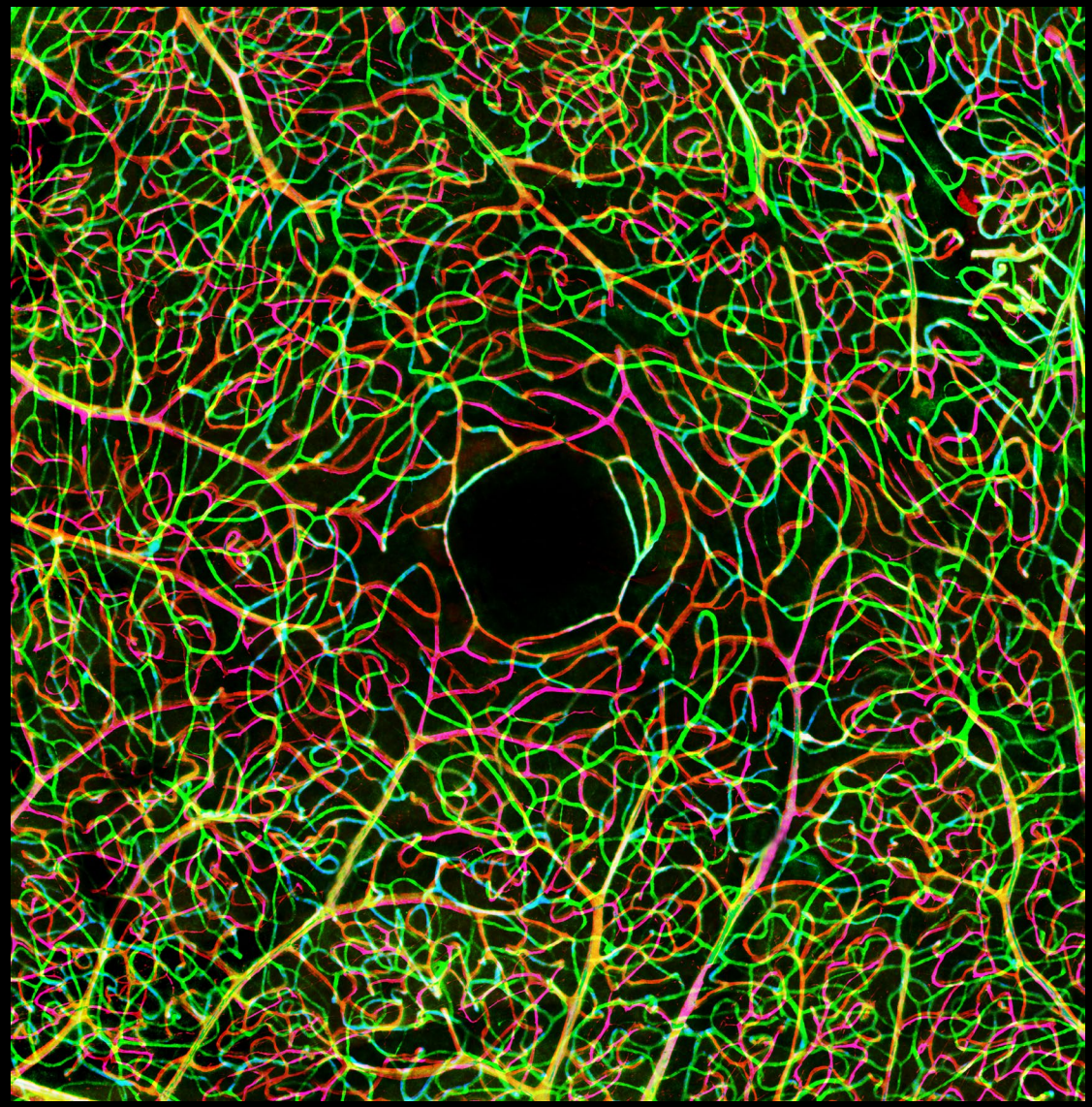

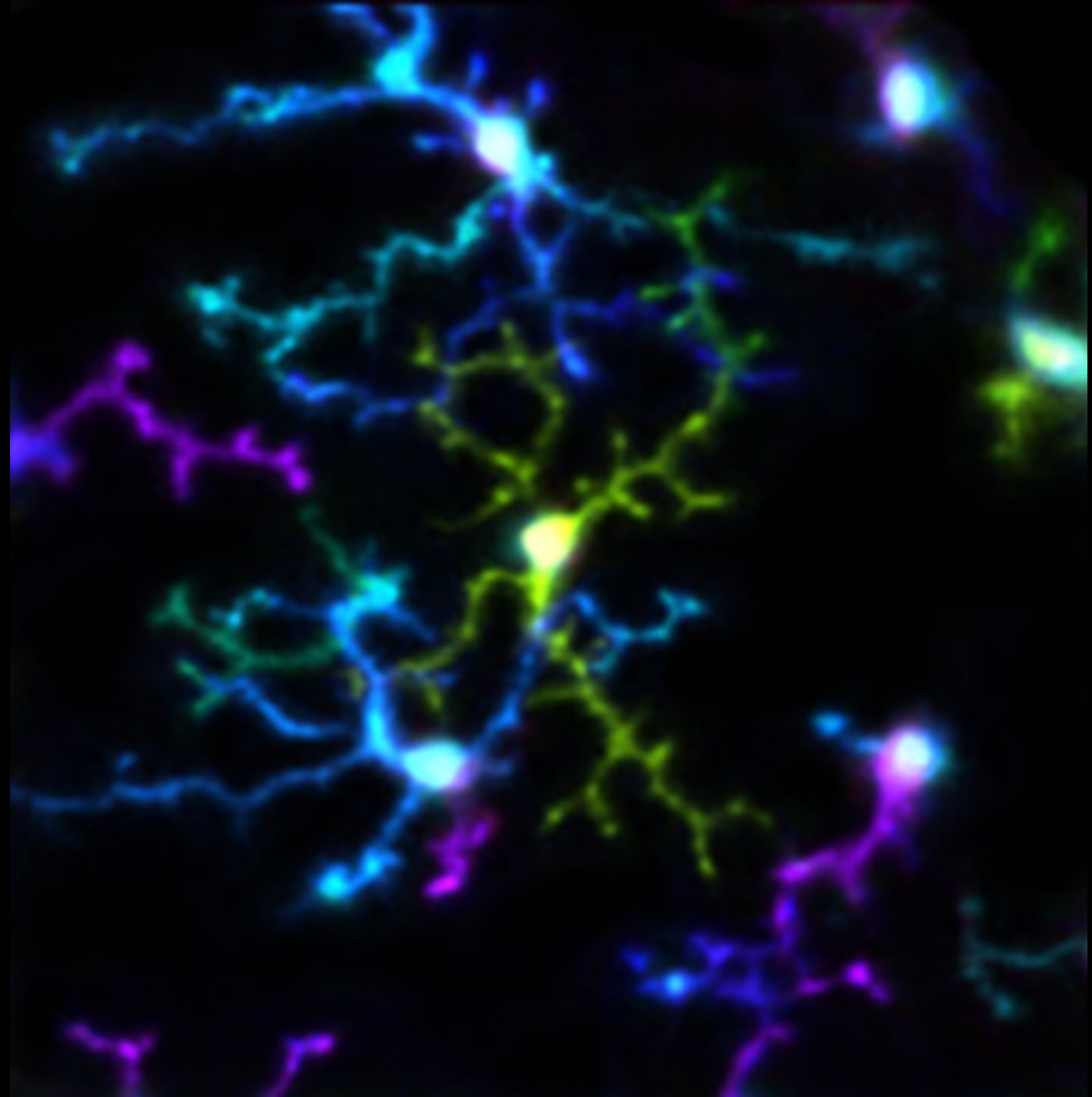

Image by
Daniel J. Wahl,
PhD

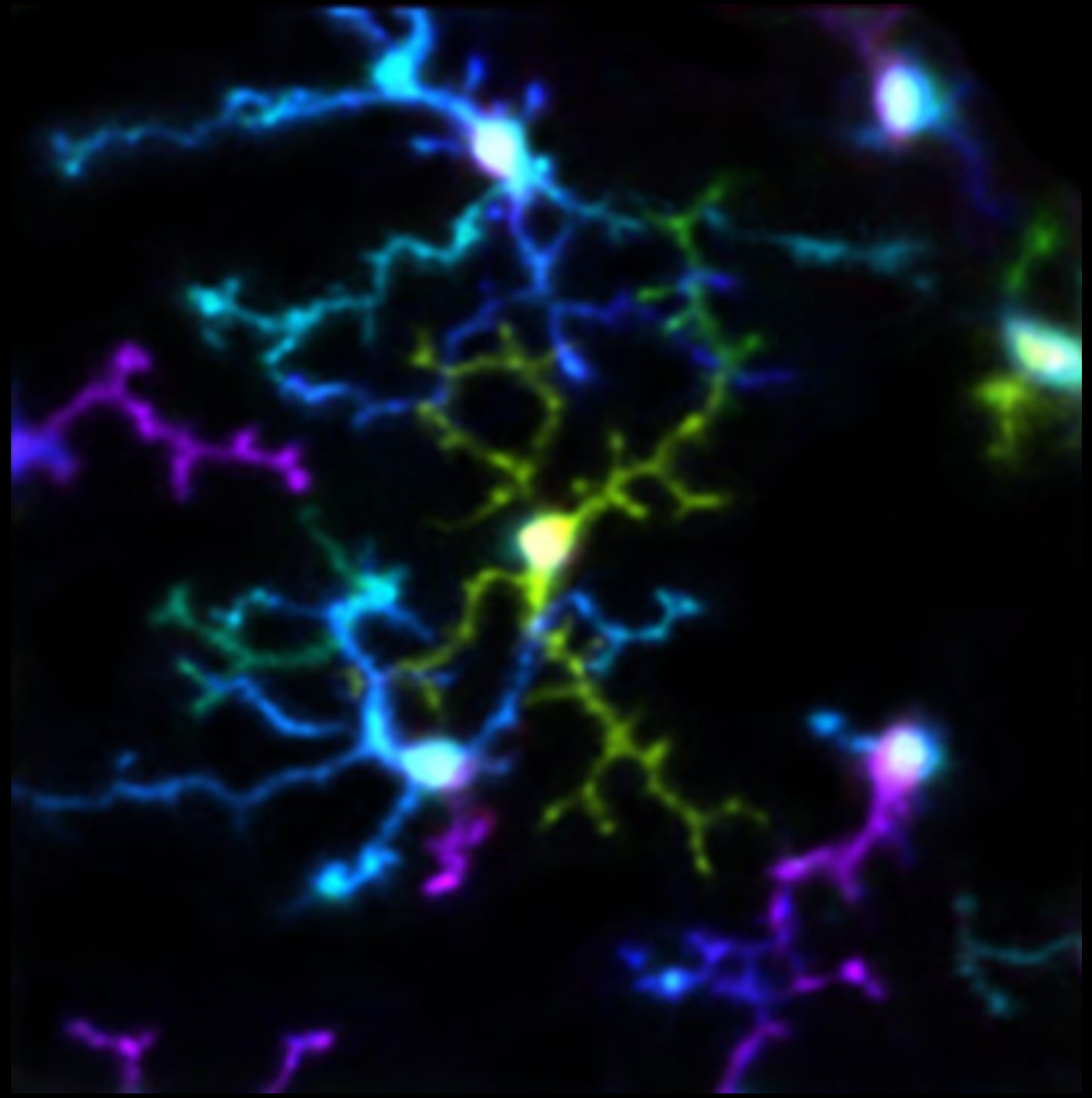

Microglia labeled with GFP and imaged throughout the inner retina of a living mouse. The image was generated with a custom-built Adaptive Optics Scanning Laser Ophthalmoscopy (AO-SLO) system. AO-SLO images were acquired at many focal positions to create a z-stack, and then composited with color to represent the depth within the retina from the outer plexiform layer (yellow) to the nerve fiber layer (magenta). Imaging microglia in vivo with high resolution allows for the dynamics of these immune cells to be visualized in action.

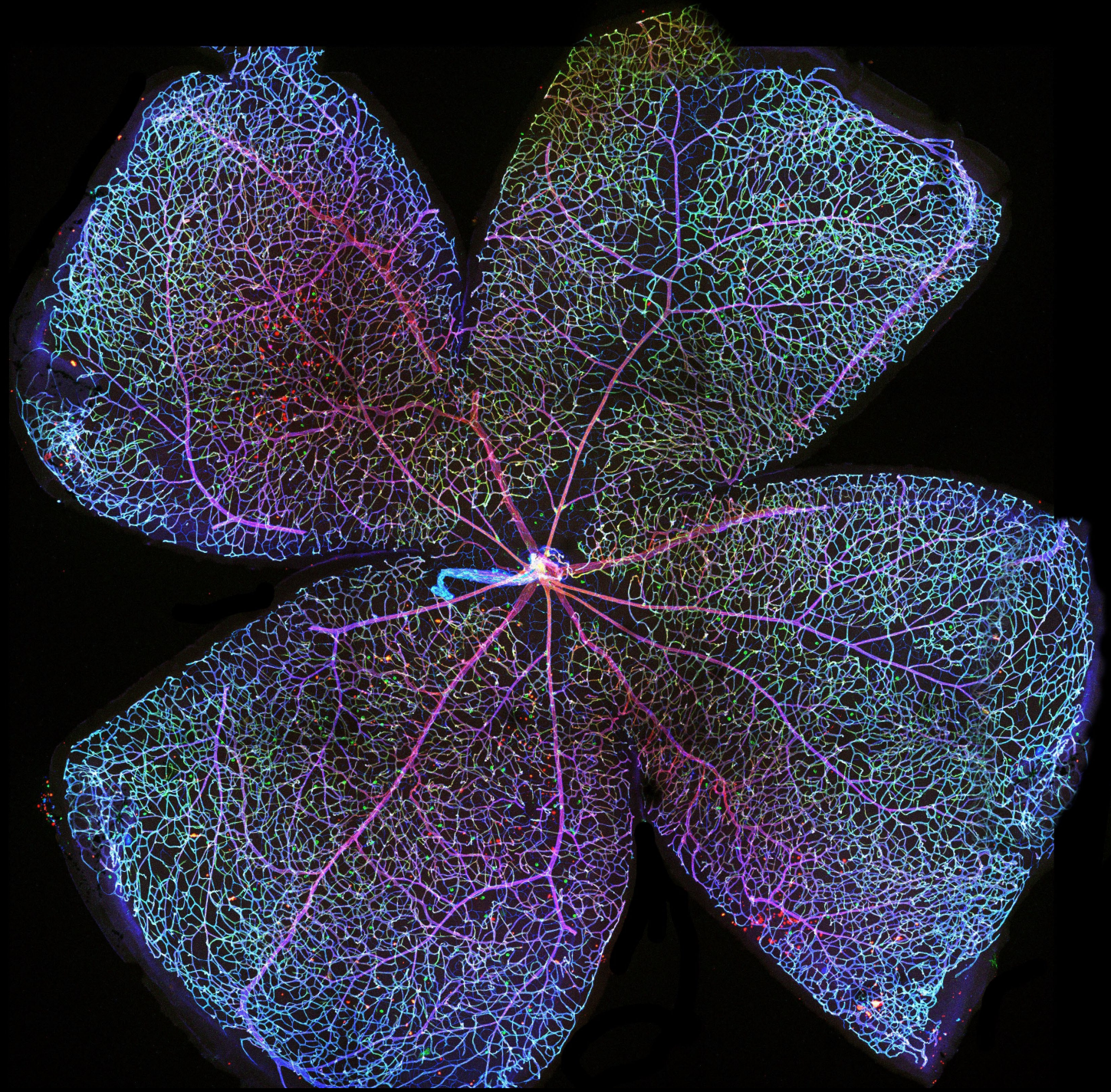

Image by David Sousa, MD, PhD; Inês Leal, MD, PhD, FEBO; and Cláudio Franco, PhD

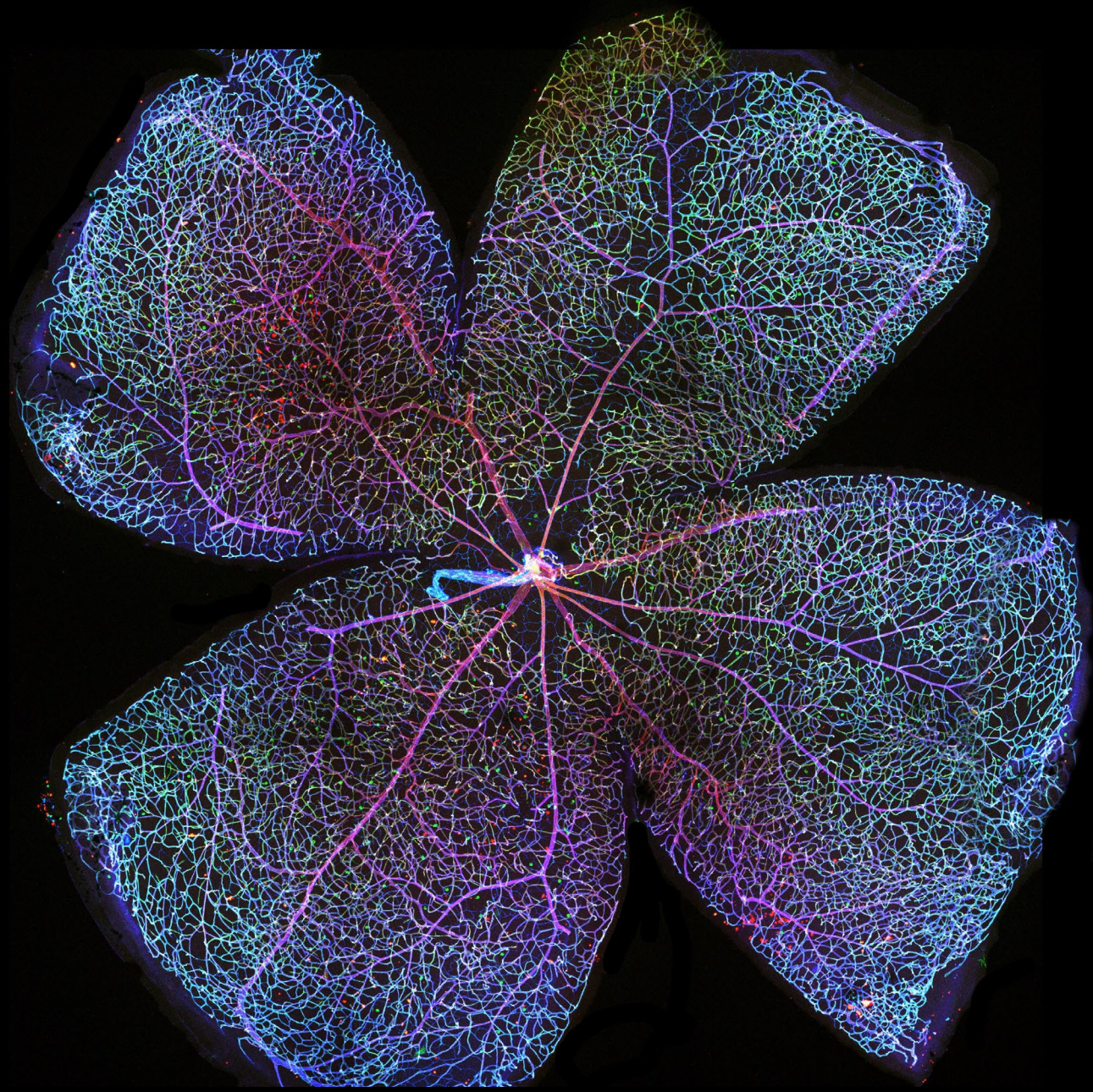

Whole-mount immunofluorescent study of retinal vessels.

A 21-day-old mouse retina was flatmounted and immunostained for collagen IV (extracellular matrix, blue), ICAM2 (vascular lumen, red) and isolectin B4 (endothelial cells, green). This technique provides a detailed view of the retinal vascular system and it is of great value in the investigation of the molecular mechanisms regulating vessel morphogenesis and function in health and disease in animal models.

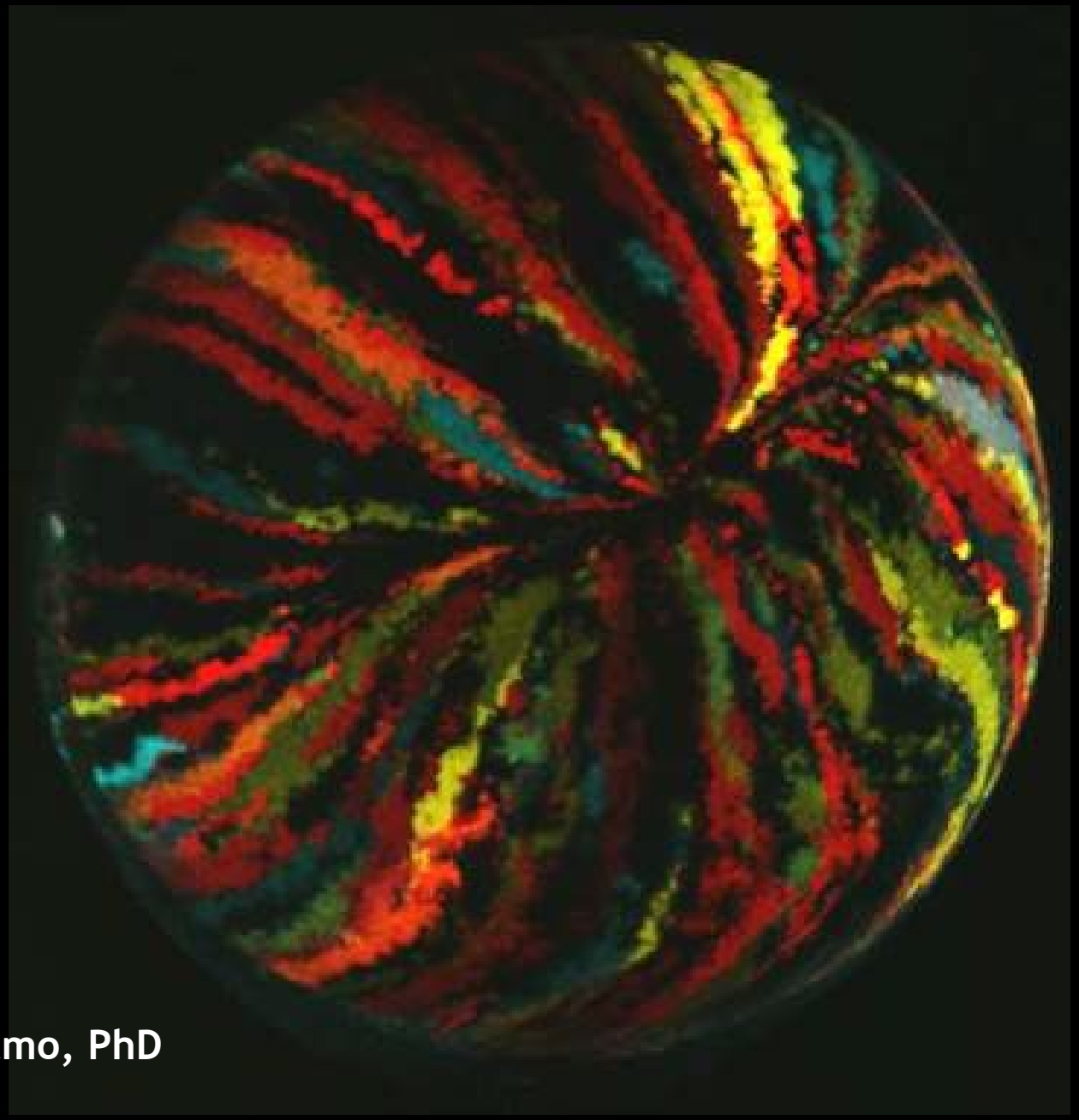

Image by Nick Di Girolamo, PhD

Attached is an image of a cornea from a 28 week old K14CreER-Confetti mouse containing the 4 color Brainbow reporter cassette. The multicolored radial streaks develop over time after induction of the transgene with tamoxifen at 8 weeks of age, and arise from Keratin 14 expressing progenitor cells which are positioned in the limbal annulus. Streaks evolve from proliferating daughter cells as they migrate centripetally from the periphery to the apex of the cornea; each represent a clone of cells that continuously replenish a narrow sector of corneal epithelia in a quasi-linear fashion. This line of research enquiry is designed to better understand the basic biology of the cornea and the dynamics and destiny of its epithelial progenitor cells under a myriad of conditions in real-time and in live animals using minimally invasive microscopy techniques.

We have previously published images from Confetti mouse corneas that have been taken on intravital and confocal microscopes (Di Girolamo et al., Stem cells. 2015;33:157-167; Di Girolamo et al. Prog Ret Eye Res. 2015;48:203-225; Richardson et al., Ocular Surf. 2016;14:82-99; Lobo et al., Nature Comm. 2016;7:123888). However, here we present the first images taken on a Zeiss Z1 Lightsheet using 4 channels (one for each fluorophore).